AN INTERPRETATION OF THE AEROMAGNATIC DATA FROM THE NORTH- CENTRAL PART OF THE CHAD BASIN IN NIGERIA.

BY

OLASUPO - ADELEKE, OYETUNJI TAHIR B.Sc
USMANU DANFODIYO UNIVERSITY, SOKOTO

THESIS SUBMITTED TO THE POST GRADUATE SCHOOL, AHMAD BELLO UNIVERSITY, ARIA IN PARTIAL FULFILMENT FOR THE AWARD OF A DEGREE OF MASTER OF SCIENCE IN APPLIED GEOPHYSICS.

DEPARTMENT OF PHYSICS,
AHMAD BELLO UNIVERSITY
ARIA - NIGERIA.

SEPTEMBER, 2000.

DECLARATION

This is an original work carried out by the author under the supervision of Prof. C. O. Ajayi. The thesis has not been submitted in whatever form to any institution, organization or body for the award of any degree.

The works of others are duly acknowledged and referenced.



OLASUPO - ADELEKE, Oyetunji Tahir

AHMADU BELLO UNIVERSITY, ZARIA
OCTOBER, 2000

CERTIFICATION

This thesis entitled "An Interpretation of the Aeromagnetic Data from the North - Central part of the Chad Basin in Nigeria" By Olasupo - Adeleke Oyetunji Tahir meets the regulations governing the award of the degree of Master of Science (M.Sc.) of Ahmadu Bello University, and is approved for its contribution to knowledge and literary presentation.

Professor C. O Ajayi
(Chairman, Supervisory Committee)

6/11/2000
Date

Dr. M. N. Umego
(Member, Supervisory Committee)

6/11/2000
Date

Professor I. B Ozasuwa.
(Head of Department)

11-11-2000
Date

Professor S. B Ojo
(Dean, Postgraduate School)

17/03/01
Date

DEDICATION

Dedicated To:

The late Bashorun M.K.O. Abiola, the indomitable 14th A'are - Ona Kakanfo of Yorubaland, whose in - describable philanthropy transcends ethnic and tribal boundaries. May his kind soul be reposed by Almighty Allah in paradise.

My indefatigable father in a million, Alhaji Bashir Oyebamiji Adeleke, who stoutly backed me throughout the period of acquiring my post - graduate degree and for his caring and fondest love to me, including his being the educational beacon of my life.

My late Mother , Madam Sidikat Asunke and my late grandmother, Alhaja Asimonwu Omoboade of blessed memory. May Allah accept them in Aljanat.

ACKNOWLEDGEMENTS

My humble gratitude goes to almighty Allah for his unquantified mercies in guiding me through this post graduate course.

My unalloyed gratitude goes to my supervisor Professor C.O. Ajayi, who closely monitored and supervised this thesis at every stage. I thank him for his suggestions, criticisms, and corrections of the manuscript. Also my gratitude goes to Dr. M. N. Umego, his fatherly and humane gesture towards the data analysis of this thesis is highly acknowledged. My unquantified thanks goes to the Head of department, Professor I. B. Osazuwa, who made my entire stay in A.B.U. during this research a memorable one. To them, may Almighty God shower His blessings on them all.

I am also grateful to the entire management and staff of Comprehensive College, Zaria. I am particularly grateful to the Director and Deputy Director, Lt. Col. A. A. Adebayo and Mrs. F. T. Adebayo for all the experience I acquired in the College through the various promotions up to the Vice-Principal level, May Allah continue to shower His blessings on them. The company and encouragement of Mrs A. O. Olorunkalu who is my confidant in the college is also appreciated.

Very big thanks to Mr. Suleiman Anka and Mr. Kola Lawal who provided the academic support for this study. The understanding and cordial relationship of Olatunji Saminu, Ibe Stephen, Zome Joseph, Pascal Ayi, Na-Allah Taiye, and David Bachama who are my friends and colleagues is appreciated.

Love of my heart, Omolara Ganiyat, the vacuum of my life that you are filling and your understanding to bear with me is highly appreciated.

The moral and material supports of my step-mother, Mrs. Simbiat Arike and my able sister, Mrs Jemidat Abidemi Oladehinde are gratefully acknowledged. My younger ones; AbdulAzeez, AbdulHakeem, Teslim, AbdulRahman, Taofik, Rashidat, Abdullahi, Ismaila, Zainab and Lukman, May Allah protect you all and give you the wisdom and zeal that will see you through to succeed in life.

The kind gesture and support of the following towards the completion of my course are immediately acknowledged; Vice-Admiral Jubril Ayinla , Oyo State Government , and Oyo- East Local Government.

I thank the member of staff of Comprehensive College, Zaria Computer Center namely: Boniface, Abiodun, Kingsley, Mrs. Adepoju and Mrs. Stephen for their various contributions in the typesetting of this work

Finally, I thank Almighty Allah for giving me the intense courage, dogged determination, and profound energy needed to complete this work.

ABSTRACT

An Interpretation of the aeromagnetic data over part (sheets 21, 22, 42, 43, 64 and 65) of the Chad Basin, which lies within longitudes 11.5° E and 12.5 ° E and latitudes 12.0° Nand 13.3° N, was carried out. A qualitative interpretation of the total field maps in the above sheets shows that most of the anomalies (source bodies) have NE - SAV alignment and few with E - W and NW - SE trends. Quantitative analyses using the Werner dcconvolution method and 2 1/2 - Dimensional modelling, using the GM - SYS program reveal, that the depth to the magnetic basement varies from 0.3 km to 2.1 km in the study area. The 2 1/2 - D modelling method revealed the presence of intrusions scattered in different places in the study area. The thickness of the intrusions range from 0.1-18 km and their lengths vary from 0.1 km - 12 km. Shapes of intrusions obtained correspond to vertical dyke of basic igneous rock as interpreted from the modelling technique. The study further suggests that the susceptibilities of the intrusions (0.0069 to 0.0092 SI Units) are greater than those of the host rock (0.0059 SI Units).

TABLE OF CONTENTS

		PAGE
TITLE		i
DECLARATION		ii
CERTIFICATION		iii
DEDICATION		iv
ACKNOWLEDEMENT		v
ABSTRACT		vii
TABLE OF CONTENTS		viii
LIST OF TABLES		xi
LIST OF ILLUSTRATIONS		xii
CHAPTER ONE: INTRODUCTION		
1.1	Location of Project Area	1
1.2	Previous Work in the Area	3
1.3	Aims of this Work	5
CHAPTER TWO: GEOLOGY OF THE PROJECT AREA		
2.1	Geology of the Chad Basin	6
2.2	Tectonic Evolution of the Chad Basin	8
2.3	Stratigraphic Succession in the Chad Basin	10
2.4	Structures in the Chad Basin	14
2.5	Geology and Structure of the Project Area	17

CHAPTER THREE: PRINCIPLES OF AEROMAGNETIC DATA AND INTERPRETATION TECHNIQUES USED.

3.1 Aeromagnetic Data..... 18
3.1.1 Magnetic Field 18
3.1.2 Susceptibility..... 19
3.1.3 Magnetic Elements..... 19
3.1.4 Rock Magnetization..... 20
3.1.5 Aeromagnetic Survey..... 21
3.1.6 Flight Pattern and Flying Elevation..... 23
3.1.7 Advantages and Disadvantages of Aeromagnetic Survey..... 24
3.2 Interpretation of Aeromagnetic Data..... 26
3.2.1 Methods of Interpretation..... 26
3.3 Interpretation Methods Used in This Work..... 27
3.3.1 The Werner Deconvolution Method..... 27
3.3.2 The Quantitative Modelling Method..... 41

CHAPTER FOUR: DATA INTERPRETATION AND RESULTS

4.1 Qualitative Interpretation (maps)..... 43
4.2 Quantitative Interpretation..... 44
4.2.1 Procedure Followed..... 44
4.2.2 Regional - Residual Separation..... 46
4.3 Profile – By - Profile Interpretation..... 50
4.3.1 Werner Deconvolution..... 50
4.3.2 Quantitative Modelling..... 53
4.4 The Depth to the Magnetic Basement Map..... 65

CHAPTER FIVE: DEDUCTIONS AND CONCLUSION

5.1 Discussion of Results..... 68

5.1.1 Trends of Magnetic Fields in the study Area..... 68

5.1.2 Types of Intrusions in the Study Area (Based on Susceptibility values)..69

5.1.3 Thickness of the Basin in the Study Area..... 70

REFERENCES..... 71

APPENDIX..... 75

LIST OF TABLES

TABLE	PAGE
2.1 Stratigraphical Succession in the Chad Basin	16
3.1 Flight Parameters in Aeromagnetic Survey	40
3.2 Werner Input Parameters	40
3.3 Model Input Parameters	40
4.1 Interpreted Model for Profile AA^{1}	57
4.2 Interpreted Model for Profile BB^{1}	60
4.3 Interpreted Model for Profile CC^{1}	64

LIST OF ILLUSTRATIONS

FIGURES		PAGE
1.1	Map of Nigeria Showing the Sedimentary Basins and the Basement Complex Regions	2
1.2	The Aeromagnetic map coverage of the Study Area	2
2.1	Geology Sketch Map of Nigeria	7
2.2	Chad Basin in Nigeria and in Surrounding Countries	9
3.1	Maximum Flight Altitude for Resolving Anomalies of Two Neighbouring Bodies	25
3.2	Standard Flight Plan for an Aeromagnetic Survey	25
3.3	Spatial Relation of 2-D Vertical Thin Dike	29
3.4	Geometry of 2-D Vertical Thin Dike	31
4.1	Total Aeromagnetic Field Map of the Study Area	45
4.2	Regional Field Map of Study Area	48
4.3	Residual Field Map of the Study Area	49
4.4	Werner Profile for Profile L211 and L 212	52
4.5	Werner Profile for Profile L178	54
4.6	Werner Profile for Profile L179	54
4.7	Magnetic Anomaly and the Depth Plot of Profile AA^{1}	56
4.8	Magnetic Anomaly and Interpreted Model for Profile AA^{1}	57
4.9	Magnetic Anomaly and the Depth Plot of Profile BB^{1}	59
4.10	Magnetic Anomaly and Interpreted Model for Profile BB^{1}	60
4.11	Magnetic Anomaly and the Depth Plot of Profile CC^{1}	63
4.12	Magnetic Anomaly and the Interpreted Model for Profile CC^{1}	64
4.13	Map of Depth to the Magnetic Basement Surface (3 – D)	66
4.14	Map of Depth to the Magnetic Basement Surface(2 – D)	67

CHAPTER ONE

INTRODUCTION

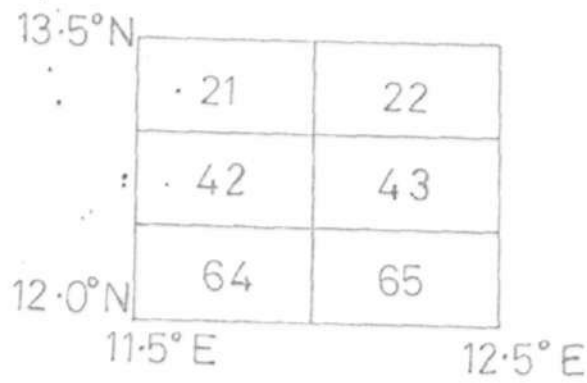
1.1 Location of Project Area.

The study area, which is in the Chad Basin, lies between longitudes of 11.5^0 E and 12.5^0 E and between latitudes of 12.0^0 N and 13.3^0 N (fig 1.1). Thus, the total map size for the study area covers 1^0 x 1.3^0 which gives approximately a land area of 15,730 km^2. There are 56 parallel N-S oriented flight lines with nominal flight line spacing of 2 km and 15 tie lines with nominal tie line spacing of 10 km in the study area. The aeromagnetic map coverage of the study area, showing the arrangement of the sheets, is shown in figure 1.2.

The Chad Basin is the largest area of inland drainage in Africa occupying about 230,000 km^2 in the Central Sahara and Southern Sudan (Barber, 1965). According to Matheis (1976), about 1/10th of the basin is situated in the north-eastern part of Nigeria, where the western limit is formed by water divide between the Niger and the Chad drainage systems while its southern limit is the water divide between the Chad and the Benue drainage systems (fig 2.2). Within Nigeria, the altitude of the basement surrounding the basin is about 530 m while, at the western margin of the basin, elevation is about 300 m along a distance of about 240 km (Matheis, 1976). This indicates a gentle slope towards the Lake Chad. This generally low - lying topography of the basin is interrupted by river channels, which extend for many kilometers (Matheis, 1976).



FIG 1·1 Map of Nigeria showing the Sedimentary Basins and the Basement Complex Regions
(After Geological Surveys of Nigeria, 1976)



21 = Sheet Number Of Aeromagnetic Sheet

Area Of Coverage = 1° X 1.5°

Fig. 1.2 Arrangement Of The Aeromagnetic Sheets Covering The Study Area.

Hydrologicaly, the rivers within the Nigerian sector of the basin generally drain Northwards towards the Lake Chad, within broad shallow valleys which only retain surface water after the heaviest rains (Matheis, 1976). The Chad Basin in Nigeria, like Sedimentary basins in other parts of the world, provides possible source rocks, reservoir beds, and the structural environment required for the formation of petroleum (Tokarski, 1973). This accounts for its possible economic potential and the present on-going geophysical surveys by oil companies, especially the Nigerian National Petroleum Corporation (NNPC), in the basin.

1.2 Previous Work in the Area

Cratchley (1960) carried out a gravity survey of the Southern part of the basin from which a Bouguer gravity map of this part of the Nigerian portion of the Chad Basin was compiled. The gravity survey maps were incorporated into the Bouguer gravity map of Nigeria compiled by Ajakaiye and Burke (1973). Also Tokarski (1973), in his work, indicated the possibility of oil and gas in the basin. He further suggested a geophysical study of the basin. Also, Yusuf (1990) carried out a detailed interpretation of the aeromagnetic data over parts of the Upper Benue trough using the Werner deconvolution technique.

The Chad Basin has attracted attention from the hydrocarbon industry as the Cretaceous sedimentary basin is formed along zones where the geothermal gradients are enhanced, and has been subsequently blanketed by the thick Cenozoic sedimentary cover

which should further enhance oil maturation (Fairhead, 1986). The concept of possible existence of petroleum in the Chad Basin has given rise to exploration activities in recent times in the Nigerian sector of the Chad Basin. The concept is based on the occurrences of oil and gas "shows" in the eastern and western parts of the Chad Basin in the neighbouring Chad and Niger Republics (Petters, 1981; Genik, 1993). This is also due to the existence of a rift which contemporaneously propagated through the Chad Basin into Libya's petroleum producing Sirte Basin (ASGA-UNESCO, 1973) and the Benue Trough. Such encouraging hydrocarbon "shows" in the Chad and Niger Republics, which are believed to be of commercial quantities (Genik, 1993) attest to a possible hydrocarbon potential in the Nigerian sector of the basin. According to Whiteman (1982), there might be prospects for hydrocarbons in structures located within the zones of marine and non-marine facies, especially in the Turonian rocks which were laid down when the south end of the Bornu Basin was connected through the Gongola Trough with the Benue Trough.

Since the late 1980s, the Nigerian National Petroleum Corporation (NNPC) has been engaged in exploratory drilling. The borehole log of some of the drilled oil wells in the Nigerian sector of the Chad Basin intercepted several layers of previously unknown igneous intrusions, which can act as structural traps for oil or channels for the evaporation of the expected accumulated oil (Ajayi & Nkereuwem, 1992).

1.3 Aims and Objectives of this Work

The present study was carried out with the primary aim of interpreting the aeromagnetic data over parts (sheets 21, 22, 42, 43, 64, and 65) of the Chad Basin using the Werner deconvolution method of interpretation and modelling of some selected profiles using a computer program known as GM-SYS. Werner deconvolution method was chosen because it enhances the recognition of most anomalies and it automatically computes their approximate horizontal locations, depths, susceptibility contrasts and geometry's (dip). The study area was chosen to carry out the objectives itemized below.

In this work, interpretations carried out were both qualitative (inspection of maps) and quantitative (model interpretations). Profile-by-Profile interpretations were carried out on all the fifty-six (56) flight lines existing in the study area. The main objective of this project is to improve the understanding of the geology of the study area using the following specific objectives:

(i) To produce a total magnetic field map of the study area in order to detect the characteristics of the anomalies present in the area; their distribution and trends, etc

(ii) To produce the regional field map of the study area with the aim of isolating the deep-seated sources.

(iii) To produce the residual field map of the study area and to interprete it.

(iv) To produce a map of the depth to the top of the magnetic basement of the study area with the aim of revealing the basement topography of the area.

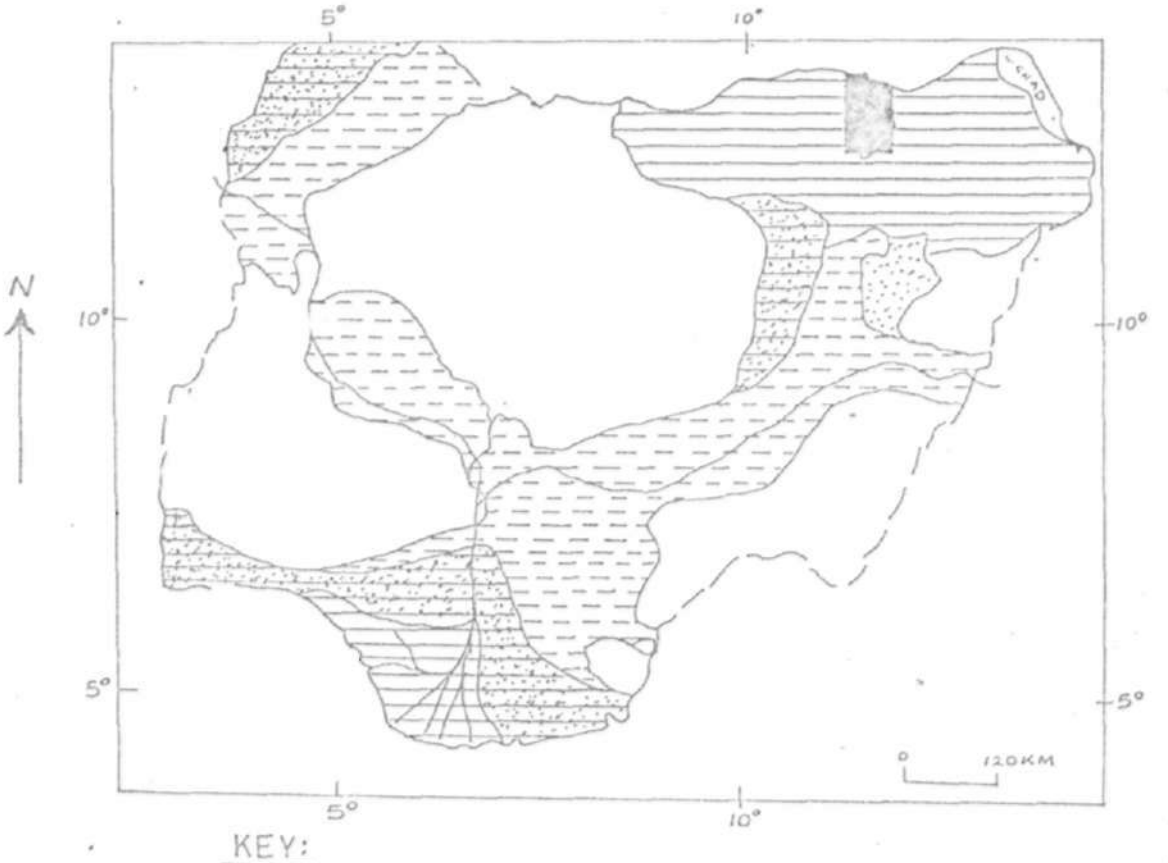
CHAPTER TWO

GEOLOGY OF THE PROJECT AREA.

2.1 Geology of the Chad Basin

The geological history of the Chad Basin in Nigeria began during the Upper Cretaceous (fig 2.1), probably uppermost Albian (Matheis, 1976). During this period, continental sandstone consisting of the Bima sandstone were deposited uncomformably on the pre-Cambrian basement mainly to the South - West margin of the basin (Barber, 1965). These events were later followed by an extensive transgression and a mixed limestone/shale sequence was deposited. The limestone/shale beds (Gongila formation) are overlain by over 530 m of marine shale (Fika formation) of Turonian to Senonian age. An estuarine - deltaic environment is thought to have prevailed towards the end of the cretaceous (Maestrichtian), at which the Gombe sandstone was deposited with intercalation of siltstones, shale's and ironstones (Furon, 1963). These sediments hardly extend Far East into the Chad basin, but they probably attained a thickness of over 320 m where they occur (Matheis, 1976).

A period of folding occurred at the end of the Cretaceous, so that the Cretaceous beds were folded into a series of synclines and anticlines that were later partly eroded creating an erosional unconformity at the base of the tertiary deposits. The Kerri - Kerri



KEY:

PRECAMBRIAN TO UPPER CAMBRIAN	Undifferentiated Basement Complex
CRETACEOUS TERTIARY	Sandstones, Coal measures, Shale; Clay Sandstone, Clay and Shales
QUATERNARY	River Alluvium, deltaic deposits and Chad formation
TERTIARY TO RECENT VOLCANICS	Basalt. Trachyte, Ryolite.
	LOCATION OF PROJECT AREA

FIG 2:1 GEOLOGY SKETCH MAP OF NIGERIA
(after Geological Surveys of Nigeria, 1976)

formation, which does not extend Far East into the Chad Basin, was deposited during the Pleistocene. The Chad Formation was deposited uncomformably on the Kerri - Kerri Formation and the older shale's belonging to the Turonian to Senonian age.

2.2 Tectonic Evolution of the Chad Basin

The Chad Basin belongs to the class of sedimentary basins related to continental plate divergence in West Africa. They are typically broad intracratonic epeirogenic basins occupying wide shallow, flat-bottomed basement down warps (Kogbe, 1981).

The Chad Basin lies within the belt of pan-African lineament defined as a zone of weakness that runs transversely from the Niger Delta to the Nile Delta (Genik, 1992). This zone of weakness is occupied by the Benue Trough in Nigeria, the Chad basin, the Kufra Basin in Libya, and the Quattara Depression in Egypt (Fairhead, 1986). Fairhead (1986) classified the basin as belonging to the genetically and physically linked system of faults and rift systems termed the West and Central African Rift Systems henceforth referred to as the (WCARS). According to him, the WCARS have two subsystems namely; the West African Rift Subsystems (to which the Chad Basin belongs) and the Central African Rift System. The WCARS spans from Mali to Kenya. The origin of the WCARS is generally attributed to the break up of Gondwanaland (fig 2.2). Results of the analysis of seismic, aeromagnetic and gravity surveys and exploration wells show that, the Chad Basin is underlain by deep rift system formed by the separation of crustal block during the Early Cretaceous as Africa and South America separated (Genik, 1992; Binks

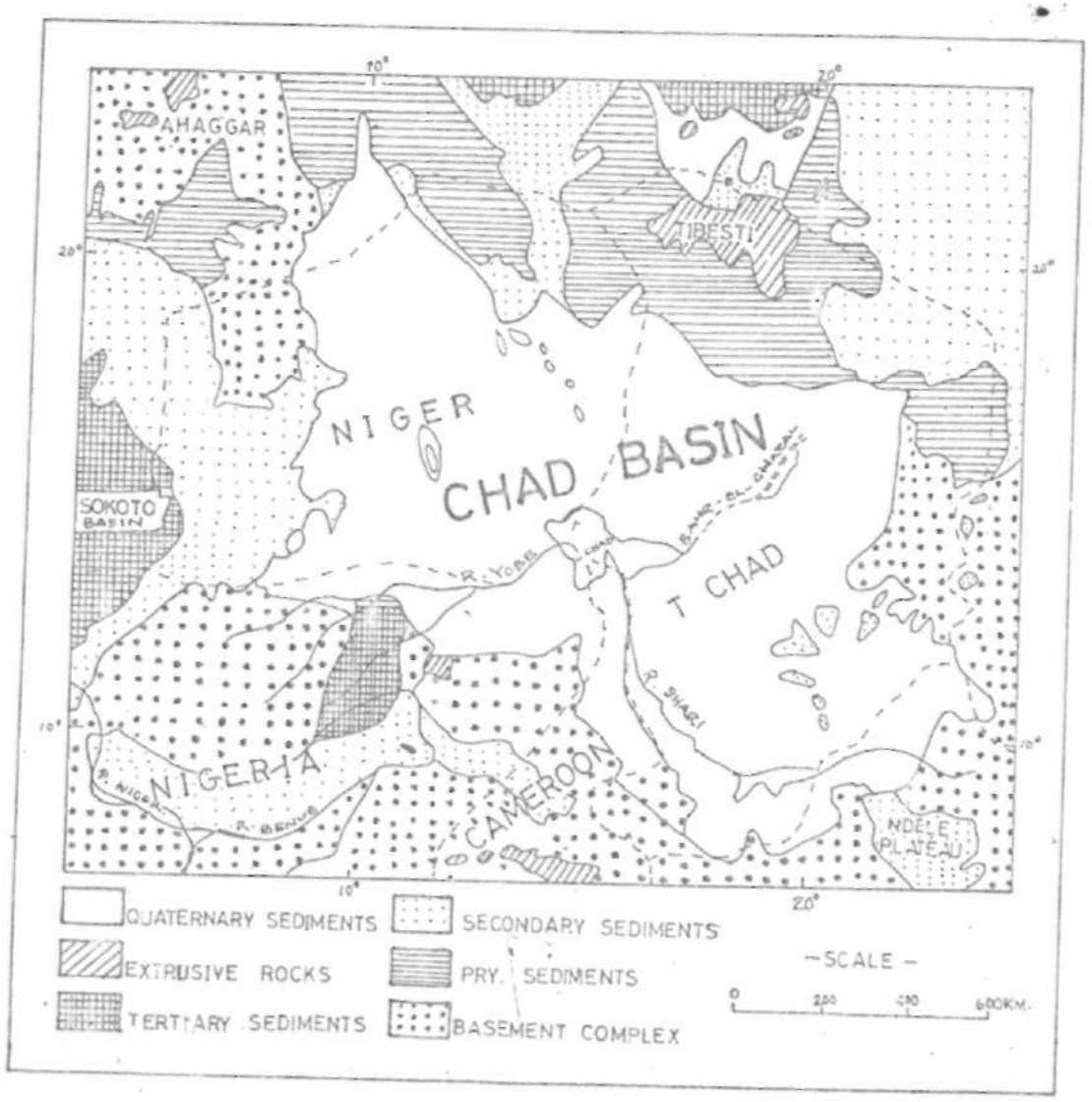


FIG 2:2 CHAD BASIN IN NIGERIA AND SURROUNDING COUNTRIES
(After W. Barber 1965)

and Fairhead, 1992). The Sedimentary Basins in Nigeria cover through the Benue Trough, Niger Delta, Nupe (Bida) Basin, Sokoto Basin, and Chad (Bornu) Basin and Dahomey Basin in the SW (fig 1.1).

The sequence of events that gave rise to the Nigerian sedimentary rocks dates back to the Pre-Cretaceous era when the uplifted continental masses of Precambrian basement rocks were unconformably overlain by Cretaceous sediments. The Cretaceous sedimentation was followed by transgression and regression of marine incursion resulting from Pre-tectonic episodes (Barber, 1965). The geologic history of the Chad Basin in Nigeria began during the Upper Cretaceous, probably Uppermost Albian (Matheis, 1976), where an estuarine-deltaic environment is thought to have prevailed towards the end of Cretaceous, these sediments hardly extend far east into the Chad Basin, but they probably attained a thickness of over 320 m where they occur (Matheis, 1976). A period of folding occurred at the end of the Cretaceous, so that the Cretaceous beds were folded into a series of synclines and anticlines that were later eroded creating an erosional unconformity at the base of the Tertiary deposits.

2.3 Stratigraphic Succession in the Chad Basin

The Chad Basin, like the Benue trough, exhibits platform sedimentation in a geotectonic setting related to rifting. As in other parts of Nigeria, there is no record of sedimentation between the Precambrian and Late Mesozoic times (Carter et al., 1963).

At large, the Chad Basin covers parts of the Northeastern Nigeria, Niger, Chad and Cameroon Republics (Fig 2.2).

The stratigraphic succession in the Chad Basin is shown in table 2.1, which gives the lithology and thickness of each formation in the basin. The stratigraphic sequence consists of six formations namely: The Bima sandstone, the Gongila formation, the Fika shales, the Gombe sandstone, the Kerri-Kerri formation, and the Chad formation.

The Bima Sandstone

In the Albian - Cenomanian period (Table 1), sparsely fossiliferous, poorly sorted medium to coarse grained continental feldsphatic sediments, called the Bima (sandstone) formation were deposited unconformably on the Precambrian Basement mainly to the Southwest margin of the Basin (Barber, 1965). The Cenomanian was characterized by extensive deltaic development, which deposited the Bima sandstone in the Chad Basin. These events were followed by an extensive transgression which deposited a mixed limestone/shale sequence (Carter et al., 1963 and Odusina et al; 1983). During the Late Cenomanian, further deepening of the sea affected the whole area and continued into the Turonian (Furon, 1963; Franks and Nairn, 1973). The marine Trans-Saharan Seaway (Kogbe, 1981) became established and allowed immigration of characteristic Tethyan faunas into the Gongola - Benue troughs and regions further to the south. Oti (1990) reported that the Bima (Sandstone) Formation is wholly continental in the northern part of the basin, while, in the Southern part of the basin, shales are found in the lower beds.

The Gongila Formation

The Bima (sandstone) formation is overlain by the Gongila formation usually regarded as transitional facies (Avbovbo et al, 1986) or passage beds (Carter et al, 1963) accompanying the marine incursion (transgression). This transgression which started in the Late Albian time peaked in the Turonian, during which the entire Benue - Chad axis became inundated by marine incursion. According to Carter et al. (1963), at the type locality of the Gongila Formation in the hill near Gongila Village (north - eastern Nigeria), it is possible to divide the formation into an upper sandstone - shale member and a lower limestone - shale member. The lower part of the Gongila formation has been dated as Cenomanian - Turonian (Popoff et al., 1986) and the Lower Turonian (Oti, 1990). During the Turonian, Fika (shale) Formation was deposited.

The Fika Shales

The Fika (shale) formation contains one or two thin impersistent limestone beds. This sedimentation, resulting from the Atlantic transgression from the South continued into the Senonian. The Turonian - Senonian depositional phase, that produced the Gongila Formation and the Fika (shale) Formation was succeeded by a regressive phase. Marine transgression in the Cenomanian - Turonian inundated large parts of Africa (including the Chad Basin reaching a maximum extent of about 80 Ma before regression led to Maastrichtian - Paleocene continental sedimentation. (Hartley and Allen, 1994).

The Gombe Sandstone

In the Late Maastrichtian time, a phase of tensional deformation occurred in the basin which continued until the end of the Cretaceous, restructuring the basin with a widespread uplift, arching along its long axis (Avbovbo et al; 1986). An estuarine - deltaic environment is thought to have prevailed towards the end of the Cretaceous (Maastrichtian), at which time the Gombe sandstone was deposited with intercalations of siltstone, shale and ironstones (Furon, 1963). These sediments hardly extend far east into the Chad Basin, but they, probably, attained a thickness of over 320 m where they occur (Matheis, 1976).

The period of folding and deformational events that followed the deposition of the Gombe sandstone are believed to have commenced in the Late Cretaceous time (Odusina et al., 1983), and resulted in the development of large anticlinal and synclinal structures in the Cretaceous rocks that were later eroded creating an erosional unconformity at the base of the Tertiary deposits (Avbovbo et al., 1986).

The Kerri - Kerri Formation

Overlying the Gombe Sandstone is the Continental (lacustrine - and deltaic - type) Kerri - Kerri Formation of Paleocene age. The Kerri - Kerri Formation is unaffected by folding but dips gently to the north and north - east below the Chad Formation (Matheis, 1976). Thus, the Chad Formation was deposited unconformably on the Kerri - Kerri

formation. There exist similarities in the structure and lithology of the Kerri -Kerri formation and the Bima Formation, the latter, however, having more feldsphatic and coarser grade sandstone (Carter et al., 1963). The Kerri -Kerri Formation appears to be derived from a terrain of Cretaceous sedimentary rocks whose relief was much more subdued than the topography at the time of deposition of the Bima Formation (Carter et al., 1963).

Chad Formation

In the Pleistocene and probably Pliocene , pluvial lacustrine clays and fluviatile sands of the Chad Formation were deposited. This formation, at least 1 km thick in the deeper part of the basin (Wright et al., 1985) is a product of erosion from the waters held into the Chad Basin accompanied by episodic and sporadic uplift and volcanism (Burke, 1976). According to Burke (1976), during the Neogene and Quaternary, about 0.5 km of sediments over an area roughly 500 km in diameter has accumulated in the Chad Basin.

2.4 Structures in the Chad Basin

The Chad Basin (like the Benue Trough) exhibits platform sedimentation in a geotectonic setting related to rifting. In the Late Maastrichtian time, a phase of tensional deformation occurred in the basin and continued until the end of Cretaceous, restructuring the basin with a widespread uplift, arching along its long axis and creating

an elongate NE-SW graven system and the formation of low frequency NE-SW folds parallel to the axis of the basin (Avbovbo et al; 1986).

Towards the end of the Tertiary and until Recent times, widespread volcanic activity occurred in the uplifted, southern and central areas. Such volcanic intrusions are essentially oriented NE-SW and localized on the Southern edge of the Chad Basin and the eastern edge of the Gongola branch (Saugy, 1987). These magmatic bodies have been identified on seismic lines and they sometimes extend to the surface (Odusina et al; 1983) and sometimes terminate below the Tertiary sediments as plugs (Avbovbo et al; 1986). Recent exploratory drilling has further confirmed the presence of these bodies in the Chad Basin (NNPC Kanadi well; rig report), while Genik (1992) reported rhyolite and basalt dykes and dolerite sills in the Sedigi and Kumai wells respectively close to the Lake Chad in the Chad Republic. According to him, these volcanics have been dated stratigraphically to be no older than 85-95 Ma. This is further supported by Ajakaiye and Verheijen (1983) who suggested progression of granitic intrusion from the Hoggar region (600 Ma) to the Jos Plateau (100 Ma). Today, sand dunes, river alluvium, deltaic and lagoonal clay flats blanket wide areas to the South and Southwest of the Lake Chad.

AGE	FORMATION	LITHOLOGY	THICKNESS (m)	AVERAGE THICKNESS (m)	DEPOSITIONAL ENVIRONMENT
Pliocene Paleocene	Chad Formation	Clay, Sand	717 – 1695	400	Lacustrine
Paleocene	Kerri – Kerri Formation	Coarse Sandstone, Claystone, Sandstone	Not Investigated	130	Continental
Maastrichtian	Gombe Sandstone	Shale, Limestone, Siltstone.	Not Investigated	315	Deltaic, Estuarine
Turonian – Santonian	Fika Shale	Blue – black Shale	840 – 1453	430	Marine
Turonian	Gongila Formaton	Shale, Limestone, Sandstone	162 – 420	420	Marine, Estuarine
Albian – Cenomanian	Bima Formation	Bima Formation	716 – 850	3050	Continental
Pre – Cambrian	CRYSTALLINE BASEMENT				

Table 2.1: Stratigraphical succession in the Chad Basin (northeastern Nigeria), after Barber, 1965; Carter et al.,1963.

2.5 Geology and Structure of the Project Area

The project Area, which covers part of the North Eastern part of Nigeria lies within the Chad Basin. A map showing the geology and extent of the Basin is shown in fig 2.2. The areas covered by sediments which gently dip towards Lake Chad and may therefore be classified as a covered shield area (Howell, 1959). The Chad Basin is underlain mainly by deposits known as Chad formation (Carter et al; 1963). The crystalline rocks which outcrop around the margin of the basin, consists of granite and flows of basalt (Barber, 1965).

CHAPTER THREE

PRINCIPLES OF AEROMAGNETIC DATA ACQUISITION AND INTERPRETATION TECHNIQUES USED

3.1 Aeromagnetic Data

3.1.1 Magnetic Field

The magnetic field strength at a point is defined as the force per unit of pole strength, which would be exerted upon a small pole of strength p_0, is placed at that point. Thus, the field strength H due to a pole of strength p, a distance r, away is:

$$H = \frac{F}{P_0} = \frac{P}{ur^2} \qquad \text{.....(3.1)}$$

The magnetic field strength is often expressed in terms of the density of the lines of force or flux representing the field. In the mksg system, the unit of flux density is the tesla, which is 10^4 oe.

3.1.2 Susceptibility

In the case of a homogenous external field, H that makes an angle, Ø with the normal to the surface of a material capable of being magnetized, the induced pole strength per unit area is

$$I = K H \cos\theta \quad \ldots\ldots (3.2)$$

And for a field normal to the surface,

$$I = K H \quad \ldots\ldots (3.3)$$

Where K, the proportionality constant, is called the susceptibility. For a vacuum and for entire nonmagnetic substances, K is zero. Magnetic materials having positive susceptibilities are known as paramagnetic. Grains of such materials tend to line up with their long dimension in the direction of the external field. A paramagnetic material of very high susceptibility may be referred to as ferromagnetic. A few substances, such as rock salt and anhydrite, have negative susceptibilities and are designated as diamagnetic. Grains of such materials tend to line up with their long dimensions across the external field.

3.1.3 Magnetic Elements

A magnetic needle that is free to orient itself in any direction around a pivot at its center will assume a position in space determined by the direction of the earth's magnetic field 'F' at that point. Since measuring instruments conventionally installed in magnetic

observatories respond only to horizontal or vertical components of the actual field, it is customary to resolve the total field 'F' into its horizontal component 'H' (separated into X and Y projections) and its vertical component 'Z'. The angle which 'F' makes with its horizontal component 'H' is the inclination 'I' and the angle between H and X is the declination 'D'. The quantities X, Y, Z, D, H, F, and I are known as the magnetic elements. The magnetic elements are related as follows:

$$H = F \cos I$$

$$Z = F \sin I = H \tan I$$

$$X = H \cos D$$

$$Y = H \sin D$$

$$X^2 + Y^2 = H^2$$

$$X^2 + Y^2 + Z^2 = H^2 + Z^2 = F^2$$

3.1.4 Rock Magnetization

The earth's magnetic field is mapped to guide our inference with regards to the structure of the earth's crust, which contains reasonable amount of ferromagnetic minerals. The crystalline rocks of igneous origin, such as granite, gabbro, and basalt contain reasonable amounts of ferromagnetic minerals such as magnetite and hematite (Telford et al., 1982). The rocks, thus, have magnetizations, which are likely to be induced by the earth's magnetic field, and are, in part, permanent or remanent. However, rock magnetization is not governed by a simple relationship. Magnetization of rocks depends upon magnetic mineral contents, type of mineral, particle size, strength, degree of dispersion and

direction of magnetic field during the formation and subsequent changes in the earth's field (Vacquire et al., 1951). Magnetization in rocks is modified by temperature cycle, stress cycle, tilting or rotation of block, chemical and mechanical alteration, recrystalization as well as addition and removal of minerals (Telford et al., 1982). This magnetization influences the earth's magnetic field above the surface of the earth to an extent that can be detected by sensitive magnetometers.

The use of aeromagnetic method in basement mapping, to determine the maximum depth of sedimentation in sedimentary basins lies in the fact that sedimentary rocks are practically non - magnetic while igneous and metamorphic rocks are to varying degrees, magnetic depending on their mineral composition. These rocks probably lose their ability to retain magnetization at some depths where their temperatures rise above a certain value called the Curie point. For most magnetic materials, the Curie point is about 500^0 C, a temperature exceeded below depths of 18 km - 27 km (Ofoegbu, 1985). In areas of high thermal gradient, this criterion has been used to delineate area with high thermal gradient from aeromagnetic data (Bhattacharya and Lue, 1975).

3 .1.5 Aeromagnetic Survey

Over seventy five percent of the Nigerian landmass has been covered by aeromagnetic survey to aid basement mapping and to guide the speculation for the search for economically viable minerals containing reasonably high amounts of ferromagnetic substances. The aeromagnetic map coverage of the study area is shown in fig 1.2. The

3.1.6 Flight Pattern and Flying Elevation.

It is customary to fly, so far, as is feasible, at a uniform elevation above sea level but within 80 m to 250 m above the earth's surface (fig 3.1). Such elevation makes it possible to avoid magnetic effects from localized near - surface sources such as structures containing iron. The flight parameters of the aeromagnetic maps used in this work are given in table 3.2. The standard flight pattern to facilitate elimination of diurnal variation and other errors such as instrument drift is shown in figure 3.2. This consists of mutually perpendicular sets of parallel lines tied together by crosslines separated from one another by a distance, which usually ranges from 8 to 20 km. The entire North - South legs are flown consecutively, after which the East - West legs are traversed (or vice versa). Adjustment for diurnal variation is determined by least squares to minimize the misclosures around the individual loops (Dobrin, 1982).

Analysis of the difference in readings at each crossing, representing the field change over a series of different time periods, allow the whole survey to be corrected for diurnal variations by network adjustment. Even though the speed of the aircraft had reduced the effect of the instrument drift and diurnal variation from the aeromagnetic data, the data still has to be corrected for diurnal variation. If there were no drift or diurnal change, the analysis of differences would add up to zero around the loop.

3.1.7 Advantages and Disadvantages of Aeromagnetic Survey.

For exploration purpose, the promising aeromagnetic anomalies are confirmed by ground survey(s). The reason for this is that the resolution of the anomalies decreases with the flight altitude. The anomalies lose their sharpness and detail at high altitude, so that it becomes impossible to separate the effects of two source bodies at depth Y and horizontal spacing X apart (Dobrin, 1982), if the flight altitude exceeds X - Y as shown in (Figure 3.1). A problem prevalent with airborne magnetic survey is the magnetic effect from iron in the aircraft engine. To overcome this effect, the magnetic element (referred to as the "bird") is towed at the end of a cable. The cable is about 24 - 30 m long in order to make the magnetic effect of the plane negligible (Dobrin, 1982). The casing of the magnetic element is streamlined for maximum stability and minimum air resistance and is equipped with fins to prevent rotation. The "bird" is usually lowered through a trap - door in the floor of the cabin after the take - off. Sometimes the "bird" is mounted on the wing tip or at the tip of the air plane's tail. When the magnetometer is attached to the plane, in which case, coil installation compensates for the aircraft magnetic field.

Another problem is to correlate all total field readings with the position of the plane at the instant they are taken. This is overcome through the use of electronic positioning system, aerial photography, and the use of Doppler system of navigation (Dobrin, 1982).

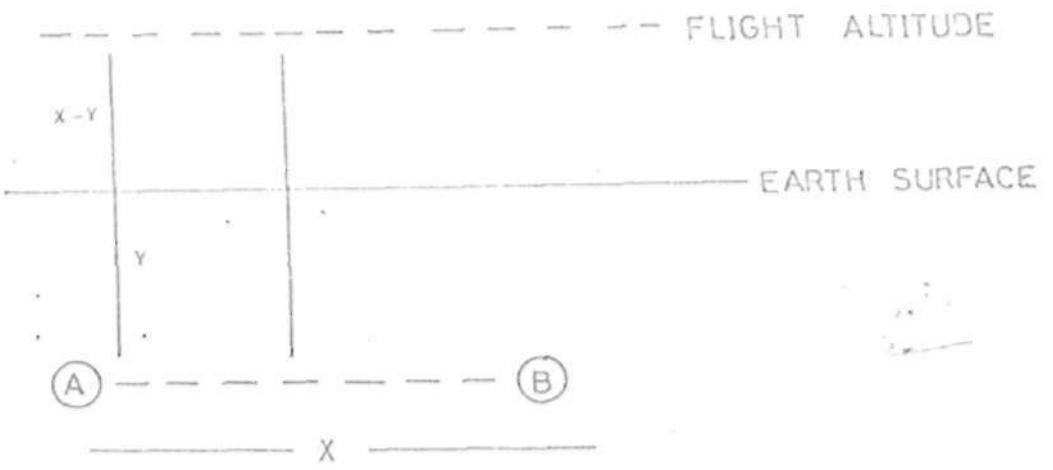


Fig 3.1 Maximum Flight Altitude For Resolving Anomalies Of Two Neighbouring Bodies, Distance X Apart. (after Dobrin, 1982)

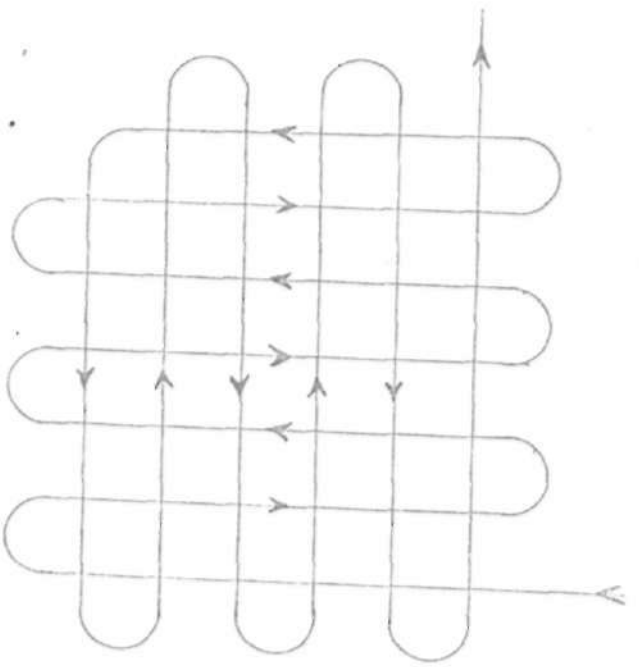


FIG 3.2
Standard Flight Plan For an Aeromagnetic Survey
(adapted from Dobrin, 1982)

Airborne magnetic surveying makes uses of an aircraft. The use of an aircraft has the following advantages:

- It makes covering a large area within a short time possible.
- It makes obtaining magnetic data from areas, which are otherwise not accessible possible.

Helicopters are more suitable than fixed wing aircraft for magnetic surveys over very rugged terrain because they can maintain more uniform elevation above the ground surface (Dobrin, 1982).

3.2 Interpretation of Aeromagnetic data

3.2.1 Methods of Interpretation

The first step in the interpretation of aeromagnetic map is qualitative, with the aim of detecting such characteristics as anomaly distribution, structural trends, etc. The next step in the interpretation technique is quantitative.

The magnetic anomalies caused by diverse model shapes, such as the thick dike of finite strike length, etc may be obtained through an appropriate numerical integration of the expression for the magnetic effect produced by a finite thin plate. Hence, various interpretation methods are in use by exploration geophysicists for the purpose of quantitative interpretation of aeromagnetic data. These methods include the curve fitting methods, which are based on a few specified points of a magnetic profile; the upward or

downward continuation methods, among others (Vacquire et al, 1951; Werner, 1953; - Gay, 1963).

3.3 Interpretation Methods Used in This Work

Apart from the qualitative interpretation (maps inspection), the quantitative methods used in this work are the Werner Deconvolution method and 2 ½ - D modelling interpretations and the regional - residual separation methods.

3.3.1 The Werner Deconvolution Method

The Werner deconvolution technique was first introduced by Werner in 1953 (Werner, 1953). The method is one which enables interpretation of aeromagnetic data to determine the depth; magnetic susceptibility and dip of the causative semi - infinite and homogenous thin sheets; whatever their strikes, dips or remanent magnetization and at any magnetic latitude (Hartman et al., 1971). The method was later shown to be applicable to contacts, edges, faults and other types of bodies (Jain, 1976; Ku and Sharp, 1983).

The usefulness of the method is expanded by the fact that the horizontal gradient of the total field caused by the edge of a thick interface body is equivalent to the total field from a thin dike. Statistical decision, numerical iteration, and a seven-point operator

were used to improve approximations of susceptibility, dip, depth and horizontal location of a given source.

Basic Principle: Consider the geometry and spatial relation due to a two - dimensional (2D) vertical thin dike (Figure 3.3). We choose the x - axis to be perpendicular to the strike of the dike, the y - axis parallel to the dike and the z - axis to be in the vertical direction. The dike is extended to infinity in both the y and z - directions. The vertical, horizontal and total magnetic fields caused by the dike can then be computed by the following equations (Talwani and Heirtzler 1964).

The vertical magnetic strength VMAG (x-, z) is given by

$$VMAG(x,z) = \iint \left[J_x \frac{2(x'-x)(z'-z)}{R^4} + J_z \frac{2(z'-z)^2 R^2}{R^4} \right] dx'dz' \quad \text{.....(3.5)}$$

The horizontal field strength HMAG (X, Z) is given by:

$$HMAG(x,z) = 2\iint \left[J_x \frac{2(x'-x)^2}{R^4} + J_z \frac{2(x'-x)(z'-z)}{R^4} \right] dx'dz' \quad \text{.....(3.6)}$$

For anomalies small with respect to the total field 'F', the total intensity anomaly is the sum of the projections of H and V along the direction of F, i.e.

TMAG (x, z) = HMAG (x, z) cos I cos (C - E) + VMAG (x, z) sin I ..... (3.7)

Where,

C = angle measured in a clockwise direction between x-axis and geographic north.

I = magnetic inclination of the main field F.

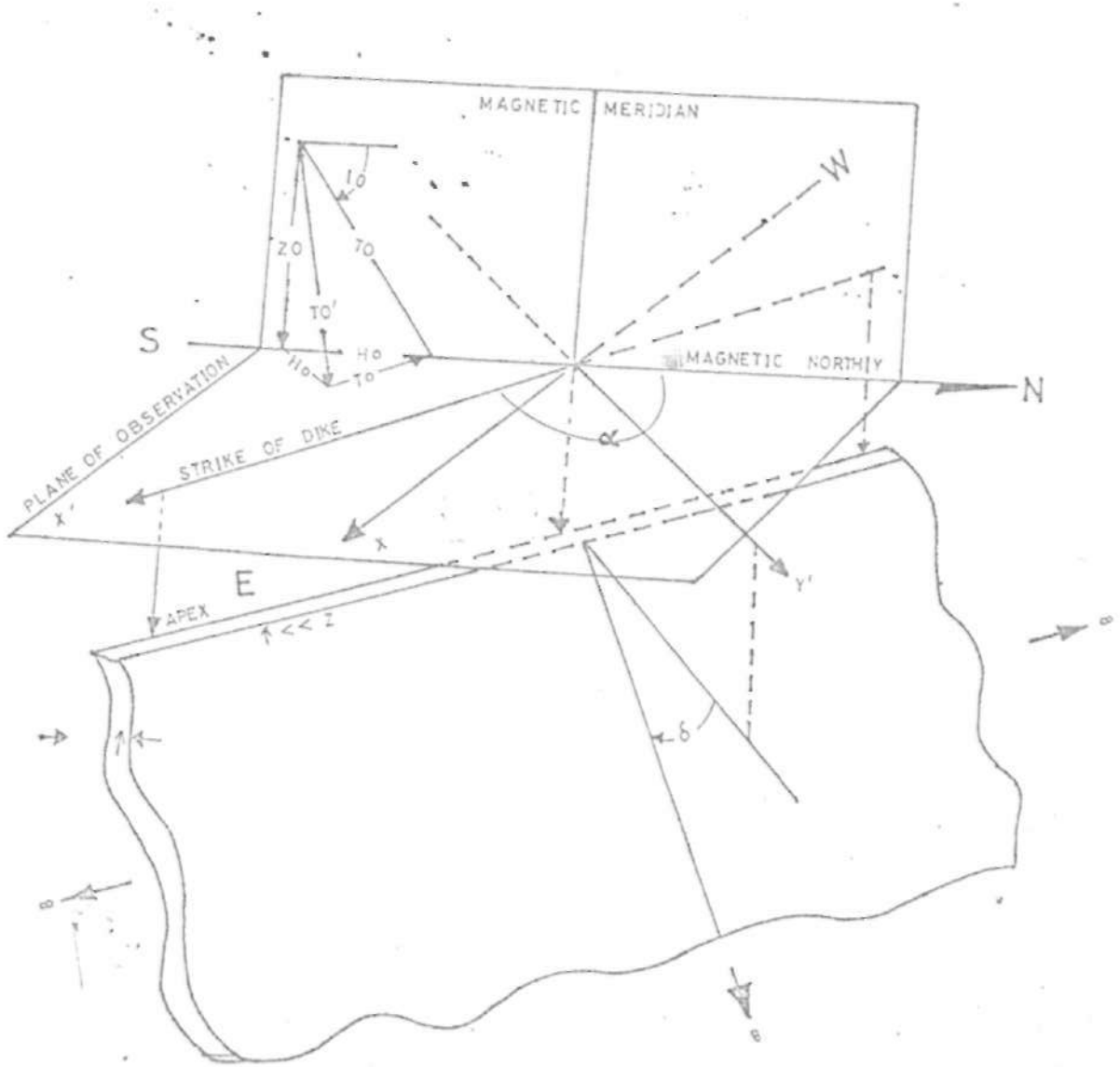


FIG. 3·3 GEOMETRY AND SPATIAL RELATION OF A THIN INFINITE DYKE (MAGNETIC SOURCE) (after Gay, 1963)

$(C - E) = \alpha$ = strike of the dike as measured from magnetic north, positive counter Clock- wise.

$J = (Jx, Jz)$ = Polarization vector.

= induced + remanent magnetization.

$R^2 = (x' - x)^2 + (z' - z)^2$

Let D be the depth to the top of the dike, and 2 ΔT the thickness of the dike (figure 3.4). When ΔT is small compared to depth D, ($\Delta T << D$), namely, the dike is thin as viewed from the point of observation at P (x, o), then a straight forward integration of equations (3.5) and (3.6) gives:

$$VMAG(x,z) = 2\int_{\Delta}^{\infty}\int_{-\Delta T}^{\Delta T}\left[J_x \frac{2(x'-x)(z'-z)}{R^4} + J_z \frac{2(z'-z)^2 R^2}{R^4}\right]dx'dz' \quad \text{.....(3.8)}$$

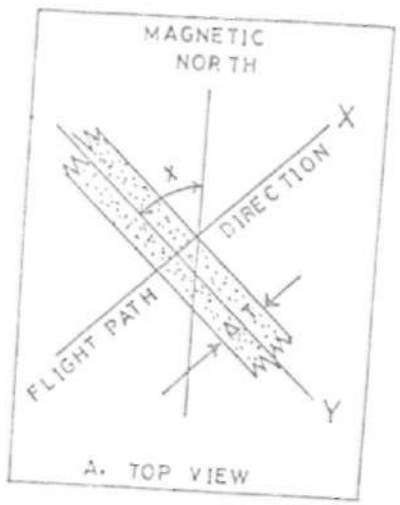
$$VMAG(x,0) = 2.2\Delta T\left[J_x\int_{\Delta}^{\infty}\frac{-2xz'dx'}{R^4} + J_z\int_{\Delta}^{\infty}\frac{\left(2z'^2 R^2\right)dz'}{R^4}\right] \quad \text{.....(3.9)}$$

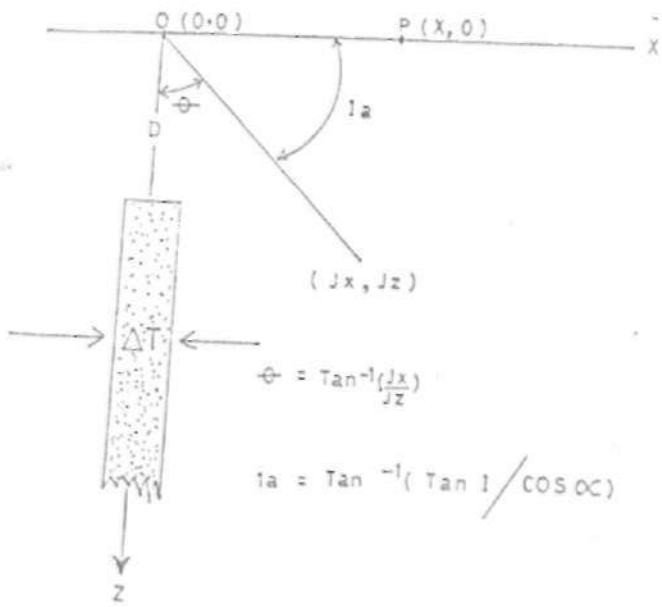
Integration of equation (3.9) yields

$$VMAG(x,0) = 2\Delta T.\frac{J_z D + J_x x}{x^2 + D^2} \quad \text{.....(3.10)}$$

Similarly, horizontal field strength is given by:

$$HMAG(x,0) = 2\Delta T.\frac{J_x D + J_z x}{x^2 + D^2} \quad \text{.....(3.11)}$$





KASIM IBRAHIM LIBRARY

FIG. 3.4: GEOMETRY OF 2-D VERTICAL THIN DIKE
(after Ku and Sharp, 1983)

To evaluate Jx and Jz, the following convention is adopted (Figure 3.4). Let the inclination of J, positive if below horizon, is represent by A. Let the angle which its horizontal projection, measured in a clockwise direction from the geographic north, be B.

Let the angle in the horizontal plane which the positive direction of x makes with the geographic north, be C, then,

$$Jx = J \cos A \cos (C - B) \quad \ldots\ldots (3.12)$$

$$Jz = J \sin A \quad \ldots\ldots (3.13)$$

F = The total field, while I and D are the inclination and declination of the earth's field respectively. Hence, sum of the projections of H and V along the direction of F is:

$$TMAG (x, o) = HMAG \cos I \cos (C - E) + VMAG \sin I \quad \ldots\ldots (3.14)$$

i.e. $$TMAG (x, o) = HMAG \cos I \cos \alpha + VMAG \sin I \quad \ldots\ldots (3.15)$$

Where $(C - E) = \alpha$

Solving equations (3.14 and 3.15) yield.

$$TMAG (x, o) = \frac{Ax + BD}{x^2 + D^2} \quad \ldots\ldots (3.16)$$

A and B are constants that depend upon the orientation and magnetization of the dike.

Where $$A = -2 \Delta T (Jx \sin I + Jz \cos I \cos \alpha) \quad \ldots\ldots (3.17)$$

$$B = 2 \Delta T (- Jx \cos I \sin \alpha + Jz \sin I) \quad \ldots\ldots (3.18)$$

Jx and Jz can be expressed in terms of A and B by solving equations (3.17) and (3.18). Hence,

$$J_x = \frac{-BV_x - AV_z}{2\Delta T\left(V_x^2 + V_z^2\right)} \quad \text{.....(3.19)}$$

$$J_z = \frac{-AV_x - BV_z}{2\Delta T(V_x^2 + V_z^2)} \quad \text{.....(3.20)}$$

Where, V_x = Cos I Cos α

Vz = Sin I

Equation (3.16) is for the total - field magnetic anomaly when the center of the dike body is located at (O, D). For arbitrary horizontal location at (X_0 , D), equation (3.16) becomes.

$$TMAG(x,0) = \frac{A(x - x_0) + BD}{(x - x_0)^2 + D^2} \quad \text{.....(3.21)}$$

It should be apparent that the main feature of Werner Deconvolution is its simplified thin dike assumption which lead to the linearization of complex non- - linear magnetic problems. This linearity is retained even when we add interference terms in the form of a polynomial $C_o + C_1x + C_2x^2$ to the total dipole field and regional gradient as follows.

$$TMAG = \frac{A(x - x_0) + BD}{(x - x_0)^2 + D^2} + C_0 + C_1x + C_2x^2 \quad \text{.....(3.22)}$$

Upon rearranging, equation (3.22) yields:

$a_o + a_1x + a_2 x^2 + a_3x^3 + a_4x^4 + b_0TMAG + b_1xTMAG = x_2TMAG$ ..... (3.23)

Where, $a_0 = - Ax_0 + BD + C_0D^2 + x^2{}_0C_0$

$a_1 = A - 2C_0x_0 + C_1D^2 + C_2D^2$

$$a_2 = C_0 - 2C_1x_0 - C_2x_0^2$$

$$a_3 = C_1 - 2x_0C^2$$

$$a_4 = C_2$$

$$b_0 = x_0^2 - D^2$$

and

$$b_1 = 2x_0 \quad \text{.....(3.24)}$$

Equation (3.23) deals with a linear problem with seven unknowns. Thus if the value of TMAG at seven appropriate points are known, the values of the seven unknowns could be obtained by solving seven simultaneous linear equations. In terms of these unknowns, we have;

$$x_0 = 0.5\,b_1$$

$$D = \sqrt{-b_0 - x_0}$$

$$C_2 = a_4$$

$$C_1 = a_3 + 2x_0C_2$$

$$C_0 = a_2 + 2C_1x_0 + C_2x_0^2$$

$$A = a_1 + 2C_0x_0 - C_1D^2 - C_2D^2$$

and

$$B = \frac{1}{D}[a_0 + Ax_0 - C_0D^2 - C_0x_0^2 \quad \text{.....(3.25)}$$

The series in equation (3.23) is intended to limit errors due to this agreement. Upon substituting A and B into equation (3.12) and (3.13), we have

$$J_x = \frac{-(2a_0 + a_1b_1)V_x - 2a_1DV_z}{4\Delta T(V_x^2 + V_z^2)} \quad \text{.....(3.26)}$$

Finally, the following results are obtained for a thin dike in real physical

$$J_x = \frac{-(2a_0 + a_1 b_1)V_z - 2a_1 D V_x}{4\Delta T(V_x^2 + V_z^2)} \quad \text{.....(3.27)}$$

dimensions in terms of the sample spacing Δx (Ku and Sharp 1983).

Horizontal position = $0.5b1\Delta x + x$ .....(3.28)

$$Depth = \sqrt{-b_0 - 0.25b_1^2 \Delta x} \quad \text{.....(3.29)}$$

$$\text{Magnetic} \sim \text{Susceptibility} \sim = \frac{\sqrt{J_x^2 + J_z^2}}{|F|}\ \Delta x \quad \text{.....(3.30)}$$

$$Dip\ angle = \tan^{-1}\left(\frac{J_x}{J_z}\right) + Ia \quad \text{.....(3.31)}$$

The computed dip angle in equation (3.31) is in relation to the projection of the total field with apparent inclination 'Ia' in the X - Z planes. But if Z - axis is parallel to the body of the dike, and the X - axis perpendicular to it, then the dip angle is given by:

$$Dip\ angle = \tan^{-1}\left(\frac{J_x}{J_z}\right) \quad \text{.....(3.32)}$$

Equation (3.32) is generally valid for a dike dipping at any angle, so long as the dike is thin in comparison to its depth. The magnetization Jz which is parallel to the body of the dike but perpendicular to the top edge of the body is called the edge magnetization, whereas the magnetization Jx which is perpendicular to the body of the dike is called the cross magnetization (Werner 1953).

Werner horizontal gradient solution can be used to determine the depth, horizontal location, dip angle and magnetic susceptibility of an interface,because the edge of a thick interface can be considered to consist of a large number of parallel thin dikes. Conceptually, the magnetic anomaly caused by the edge involves an integration of the magnetic anomaly from a thin dike, if we take a differentiation in the from of a horizontal gradient, then the differentiation and the integration cancel and we end up with the same expression for the magnetic anomaly from a thin dike. (Ku and Sharp, 1983). This implies that the horizontal gradient of the total field caused by the edge of a thick interface body is equivalent to the total field caused by a thin dike.

From Fourier transform theory, the computation of the horizontal gradient from the total field is simply a high - pass-filtering operation with a multiplication factor of iw in the frequency domain, where $i = \sqrt{-1}$ and w is the angular frequency. This means that, in addition to the original total field spectrum being multiplied by the factor w, there is also a 90 - degree phase lag in the spectrum of the computed horizontal gradient with respect to the spectrum of the original total field.

The Computer Program: A computer program known as Werner's program available in the Physics Department, A.B.U, Zaria was used to interprete the evenly spaced digitized data on each of the 56 profiles covering the project area in accordance with equations (3.18) through (3.28). The program uses seven points at regular intervals as a "window" to compute the depth, the horizontal location, the dip and

the susceptibility of the source (or edge). The "window" defined by these seven points formed the "Werner operator" that was moved along each profile at one point interval.

The detection of an anomalous source is related to the size of the "operator window". A deep source, with an associated broad magnetic anomaly, needs a Werner operator of comparable size to recognize it.

The digitized aeromagnetic data are smoothed with a running Hanning window: thereby, filtering the data to minimize "aliasing" effects caused by increased interval. The range of depths, which can be interpreted accurately, is related to the window lengths. The net effect of filtering implicitly in the selection of sample interval and of the consistency tests in solution is to minimize the appearance of interpretation from noisy data in the final plot. The presence of the high frequency anomalies, even of limited extent, mask interpretation of anomalies of comparable magnitude originating from deeper sources.

Assuming, we have an appropriate Werner operator whose size is comparable to the size of the anomaly, when we sweep the operator across the anomaly, it will be observed that a group of continuous solutions, as wide as the anomaly, are obtained when the operator straddles the anomaly. In fact, the variation may be so large that we must discard some of the solutions as our rejection criterion (weighting factor). If thin dikes are present; their anomalies are recognized from the total field data and edges are analyzed from the computed horizontal gradient of the total field (Ku and Sharp, 1983).

When the Werner operator is small, compared with the anomaly size, the operator will "see" only a small and, hence, nearly linear portion of the magnetic anomaly. As a result, it would yield a depth solution, which is much deeper than the true depth. On the other hand, if the operator were too large, the operator would very likely "see" multiple peaks from adjacent anomalies (Ku and Sharp, 1983). Thus, the desirable operator size should actually be from one - half to full - size of the magnetic anomaly under deconvolution (Ku and Sharp, 1983). In general, the optimum size of the Werner operator should be of the same order of magnitude as the anomaly size such that the operator is small enough to "see" only a single peak (or trough) yet large enough to cover sufficient variations in slopes or curvatures in the magnetic field, and at the same time, give reliable computational results (Ku and Sharp, 1983).

If we apply the Werner operator to the computed horizontal gradient, we expect that the Werner horizontal gradient should be shallower in depth because of its high frequency content, and it should be perpendicular (90 degree phase lag) in dip angle to the Werner total - field solution (Ku and Sharp, 1983). The higher order terms in the form of a seven-point operator or at least a six-point operator are needed in order to see a magnetic anomaly accurately as well as to reduce interference from the main dipole field and regional trends which are generally not of exploration interest.

In this work, as earlier stated, the Werner Deconvolution technique was applied to fifty-six (56) profiles in the study area. The aeromagnetic maps used were sheets 21, 22, 42, 43, 64, and 65. They were digitized at an interval of 0.5 km along each flight line

in each of these maps. The flight line spacing used during the survey is 2 km. The profiles are labeled as L 173, L 174, ... L 226, and the flight parameters used in the survey are given in table 3.2. The closeness of the profiles makes it possible for an anomaly to be crossed by more than one profile; thus making the correlation of anomalies from one profile to another possible.

In order to see the pictorial representation of the source body clearly, a sampling interval of 0.5 km was used. The Werner's program used for the Deconvolution was able to reduce the digitizing interval to 0.25 km using linear interpolation in order to reduce the width of the smallest seven - point Werner operator to 1.25 km. The Werner operator lengths used in this work varied from 1.25 km to 25 km in steps of 1.25 km. The typical input parameters for the computer program used in this work is listed in table 3.1 below.

TABLE 3.1: Typical Input Parameters for the Werner Deconvolution Program Used in this work

Title of Profile	= L 173
Number of data points	= 301
Sampling interval	= 0.5 km
Starting Werner Interval	= 1
Maximum Werner Interval	= 10
Minimum number of consistent depth solution acceptable	= 2.
Angle of Inclination	= 40
Angle of Declination	= 30
Total Magnetic Intensity Background of the Study Area	= 34000 nT

TABLE 3.2 Flight Parameters of the Digitized Aeromagnetic Maps

Flight line direction	= 0^0 / 180^0
Tie line direction	= 90^0 / 270^0
Nominal flight line spacing	= 2 km
Nominal tie line spacing	= 10 km
Nominal flying altitude above M.S.L	= 0.762 km

Table 3.3 Typical Model Input Parameters for Profile AA'

Profile length	= 60 km
Model depth	= 18 km
Model azimuth	= 480
Spacing between stations	= 0.5 km
Number of magnetic stations	= 12
Inclination of earth's magnetic field (FI)	= 40
Declination of earth's magnetic field (FD)	= 30
Intensity of earth's magnetic field (H)	= 34,000 nT

3.3.2 Quantitative Modelling.

Once we have obtained the Werner solutions from analysis of the total field and horizontal gradient curves, we can conveniently use the solutions as initial estimates for further refinement by GM - SYS modelling.

Quantitative modelling of the aeromagnetic data along the profiles was done in this work using the GM-SYS program. This program is an easy interactive program that can be used for modelling geological bodies of 2 - D or 2½ - D cross-section. It has the ability to quickly calculate and display the magnetic response from the cross-section of the source body as well as the cross- sectional view of the causative body concerned.

Two - dimensional modelling assumes that all bodies in the earth model are prisms extending to infinity in the strike direction; i.e. perpendicular to the line of the profile (Talwani et al., 1959). While this is a valid approximation for many geologic situations, it breaks down in close proximity to faults, dikes, and other three-dimensional feature (Rasmusen and pedersen, 1979). On the other hand, two - and - a - half - dimensional modelling permits one to limit the extents of the prisms in the 'y' direction, where the y - axis is in the strike direction. This allows the model to closely approximate many three - dimensional structures. In the modelling exercise, attempts are made to attain the "best fit" between the observed and the calculated anomalies. The model input parameter for Profile $AA^{/}$ is shown in table 3.3

Basic Principle of the Modelling Program: The equations used to calculate the magnetic response for the 2-D bodies model response are based on the methods of Talwani et al., (1959; 1964) and the algorithm used was that described by Won and Bevies (1987). The two and one half - dimensional calculations are based on the equations obtained in the work of Rasmussen and Pedersen (1979). In using the program GM – SYS, stations (points at which magnetic values were observed and calculated) must be outside the source material (i.e. they must be in an area outside the model where the magnetization or susceptibility value is equal to zero).

CHAPTER FOUR

INTERPRETATION AND RESULTS

4.1 Qualitative Interpretation

The qualitative interpretation of aeromagnetic maps is carried out primarily to detect the gross characteristics of the magnetic field over the study area and to also deduce the anomaly distribution and structural trends, etc within the study area. However, the information that can be deduced from a survey is considerably increased if some geologic information is already available.

Figure 4.1 shows the total field aeromagnetic map over the study area. Inspection of the map shows that most of the closed contours in the west and eastern portions of the map are aligned and elongated in the E - W direction. This is an indication that the source of each of the anomalies may be a dike in which the direction of elongation most possibly indicates the strike of the dyke. Some anomalies at the SW and NW edge of the map are more or less elliptical in shape suggesting the presence of structural trends along the long axis of the ellipse and their trends are NE - SW. A careful study of the magnetic anomalies discloses two clear trends. These are:

(i) The Northeast - southwest (NE -SW) trends, found mostly in the SW portion of the area.

(ii) The East - West (E - W) trend which are few and found in the central part.

(iii) A few NW - SE trends found in the SW portion of the area.

Towards the SE edge of the total field map, one can see a complicated distribution of short wavelength anomalies (i.e. anomalies which are small in widths, about 0.7 km) as opposed to those of moderately long wavelength distributed at the central and top left regions of the map. The short wavelength anomalies located at SE edge of the map with complicated distributions suggests that the magnetic sources are shallower, and their smaller widths is a pointer to smaller extent of their causative magnetic bodies. Thus, from figure 4.1, it is clear, however, that the shallow magnetic sources are having limited strike lengths and steep dips. Their susceptibility contrasts is large as well with values ranging from 0.0067 SI Unit - 0.0092 SI Unit. The Northern edge of the map is a boundary between Nigeria and Niger Republic. High average magnetic susceptibilities are normally found in bodies with mafic to ultralmafic composition commonly associated with igneous rocks.

4.2 Quantitative Interpretation:

4.2.1 Procedure Followed

In the qualitative interpretation earlier discussed, effort was made to describe the pattern of the aeromagnetic field over the study area and to infer from the total field map, the presence of structures in the area. On the other hand, the quantitative interpretation

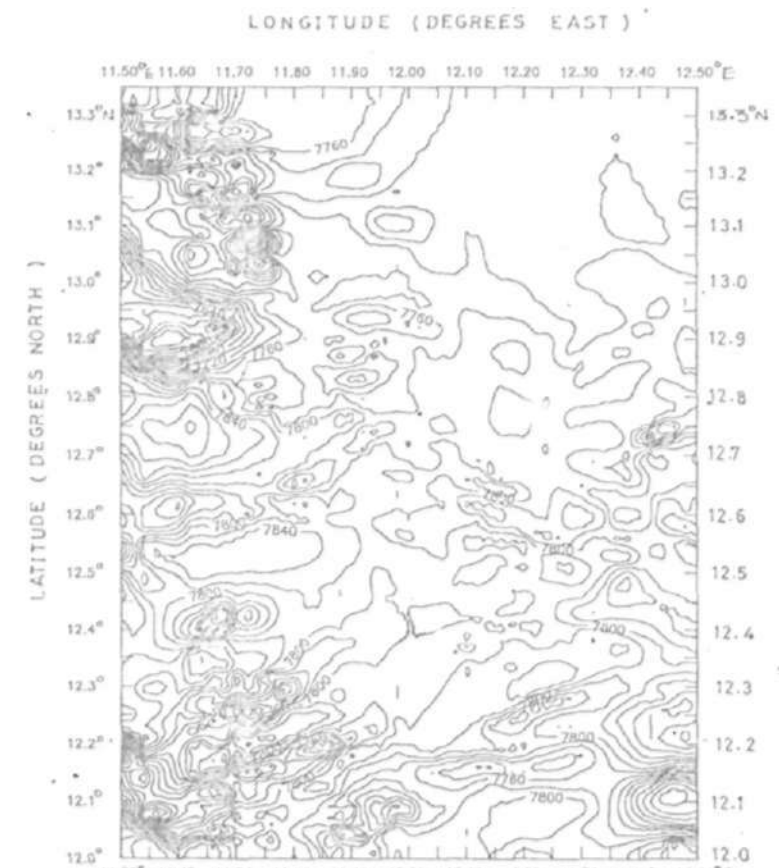


FIG. 4.1 TOTAL FIELD INTENSITY MAP OF THE STUDY AREA

(to obtain the actual field value add 25000 nT to Contour value, Contour interval is 20nT)

was carried out to determine the parameters of the source (causative) bodies such as their depths, dips, widths, and susceptibility contrasts.

4.2.2 Regional - Residual Separation

The potential field observed over an area is a combination of a regional component and a residual component. The regional component is that component of the total field caused by deep - seated sources while the residual component of the field is that component due to relatively local sources. In processing field data, one of these components (usually the regional) and then the other, i.e. the residual component, is obtained by subtracting from the measured field values of the estimated regional field at corresponding points.

The most common and flexible technique used for determining the regional component of the observed (total) field is to fit a low degree polynomial to the measured magnetic field data using the least squares method (Dobrin, 1982). Sources of regional magnetic variation in sedimentary areas include large - scale deep - seated structural features, and susceptibility effects caused by intra-basement lithological changes. Regional gradients like these often distort or obscure the effects of relatively near – surface structures such as salt domes or buried ridges. The polynomial fitting method presupposes that the residual field has a normal (Gaussian) distribution. However, in field data, many points do not fit this presumed Gaussian model. These data points which do not fit the normal distribution model for least - squares estimation. These cause

a distortion of the regional field fitted to the data by the least-squares method (Kangkolo et al, 1994). The influence of the deviatory field points can be suppressed by using the robust estimation method of Kangkolo et al, (1994). In the method, coefficients of the polynomial equation are obtained by minimizing the absolute deviation of the field values at the data points using the robust polynomial fitting of degree one (10 fitting).

The observed data set are used to compute, usually by least squares, the mathematically describable surface giving the closest fit to the magnetic field that can be obtained within a specified degree of detail. This surface is considered to be the regional magnetic, and the residual is the difference between the regional field thus determined and the total magnetic field. In practice, the surface is expressed mathematically as a two - dimensional polynomial of an order that depends on the complexity of the regional field, a first - order surface is of the form

$$Z = Ax + By + C \qquad (4.1)$$

Where A, B, C are constants and Z = regional surface.

Using the method of least squares, the values of the Coefficients A, B and C obtained for the total data set were

A = 7802.288

B = 8.72602

C = - 44.12617

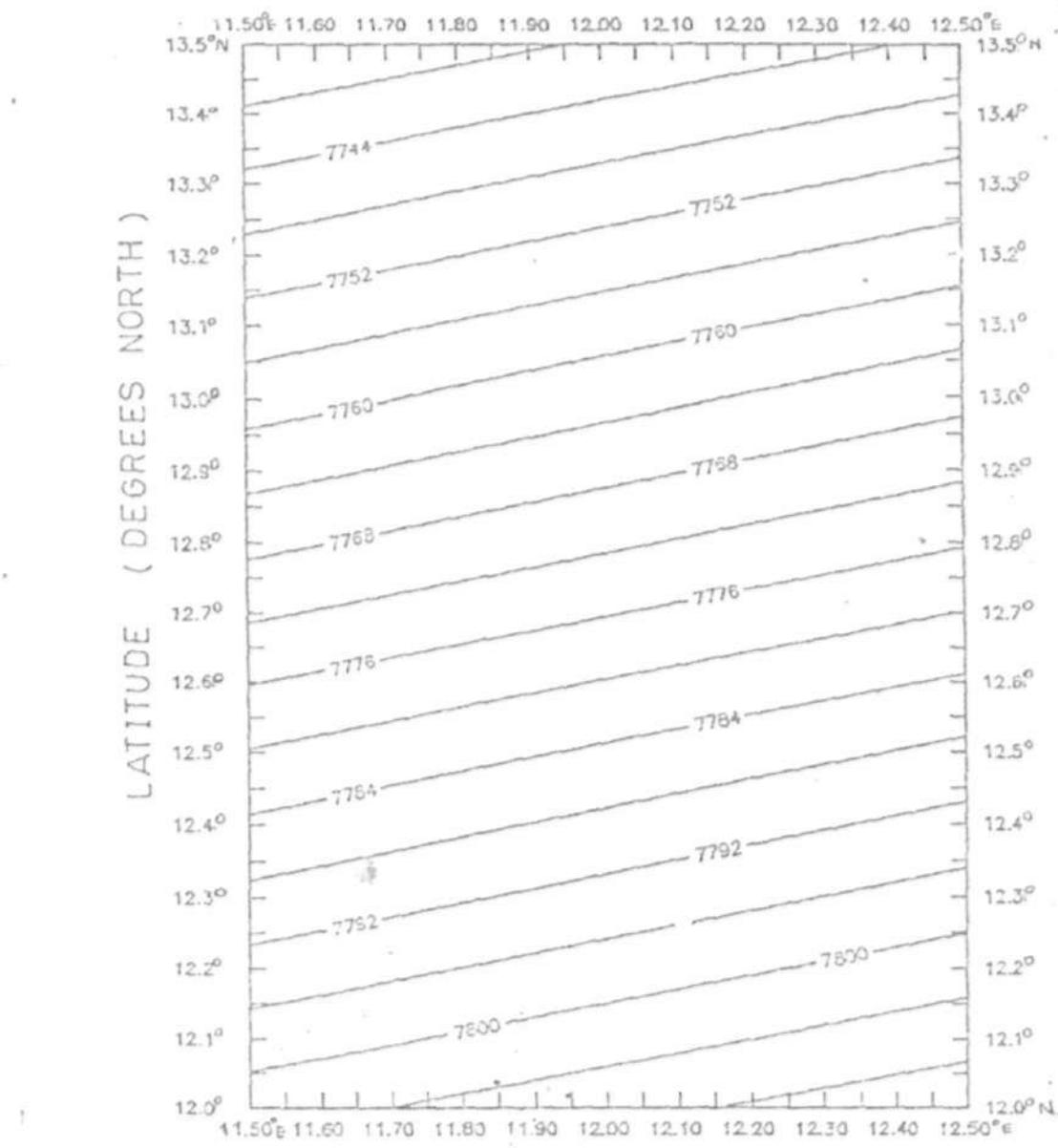


FIG. 4·2 REGIONAL FIELD MAP OF THE STUDY AREA.
(to obtain the actual field value, add 25000 nT to contour value. Contour interval is 4nT)

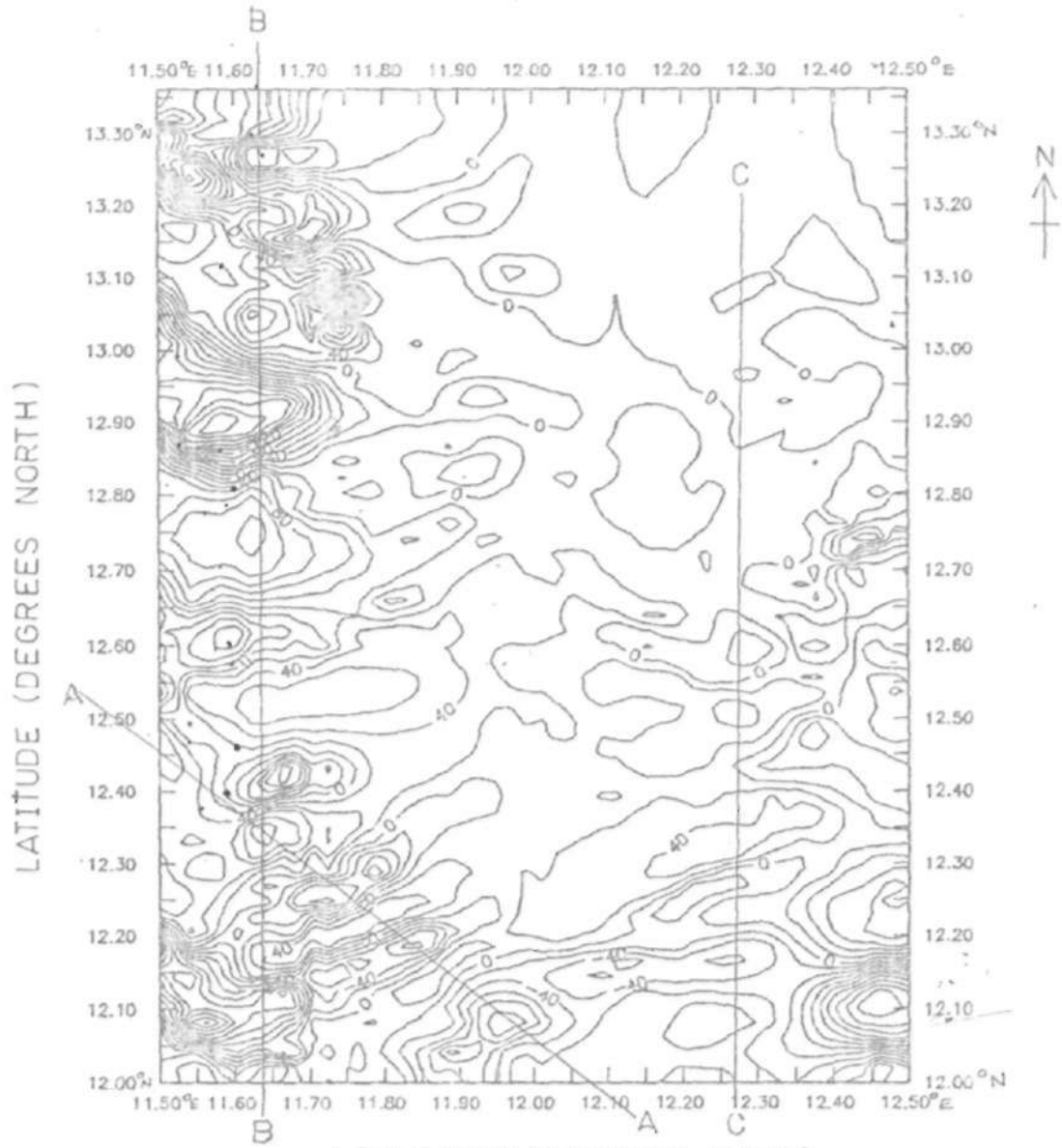


FIG 4-3 RESIDUAL FIELD MAP OF THE STUDY AREA (cont int 20nT)

Scale 1:100,000

A plot of regional field with the above coefficients is shown in figure 4.2, showing a trend of NE - SW. The residual function R for the observed magnetic field is of the form:

$$R = G - Z \quad \text{..... (4.2)}$$

Fitting a linear or higher order interference term to an anomaly reduces its amplitude substantially, and this makes the analysis of the residual very susceptible to noise (Ku and Sharp, 1983).

4.3 Profile -By- Profile Interpretations

4.3.1 Werner Profiles

The Werner profile derived for each profile by applying the Werner deconvolution to the total field data along the profile was examined. This was used to obtain a rough estimate of the depth to the top of the magnetic basement (i.e. the maximum sediment thickness) and the presence of associated structures such as intrusions and faults. The results obtained are as briefly described below.

Werner Profiles for L 211 and L 212

Figure 4.4 shows the interpretations of the Werner profiles as obtained for Profiles L 211 and L 212 (i.e., flight lines 211 and 212 of the project area respectively). These profiles are used to illustrate how adjacent profiles are correlated. Each of the profiles is 120 km long and show substantial scatter in the depth solutions. They do not yield enough solution to enable a basement surface to be adequately fitted because there is no consistency in their depth solutions. Although, considerable interpolations between solutions were required to obtain these surfaces, the interpreted inferred basement surface (dashed lines) show significant variations from profile to profile because a feature highlighted in a profile were masked in another profile.

Werner Profiles for L 178 and L 179

There is clustering of depth solutions in Profiles L 178 and L 179 thereby confirming the consistency of the solution and the presence of magnetic body (intrusion). Consistent depth solutions were observed in Profiles L 178 and L 179 as shown in figures 4.5 and 4.6 respectively, they represent a set of profiles with similar magnetic features. The profiles are each 140 km long and show substantial clusters of total field and horizontal gradient solutions. Thus, for the magnetic anomaly occurring at horizontal distance of 42 km from the southern limit of the profile, the depth to the top of the causative body in both Profiles varies from 4 km to 2.1 km in figs 4.5 and 4.6 respectively.

For example, the intrusion that appears to be buried at depth of 4 km in figure 4.5 appears to exist at a much shallower depth of 2.1 km in figure 4.6. While, for the adjacent Profile L 179, the anomaly occurring at horizontal distance of 65 km from the

southern limit of the profile has its depth to the top being 1.5 km in figure 4.5 appears to be at a depth of 2.2 km in figure 4.6. Significant clusters of solutions associated with this magnetic anomaly vary slightly in their distances and depths of occurrence. Thus, by comparing the calculated depths of depth to the top of causative body for adjacent profiles, a magnetic basement surface that is representative of the profile across the same anomalies is produced. The surface gives a close approximation of the depth to the magnetic basement and hence the maximum thickness of the sediments. The geometry of the inferred magnetic basement surface makes it possible to infer or deduce the presence of structures associated with the basement underlying the study area. The magnetic basement surface MM' fitted to the profiles is consistent for given set of profiles e.g. in profile L 178 and L 179, the consistent depths recorded for profiles L 178 and L 179 vary from 1.0 km to 2.2 km for a body located at an horizontal distance of 42 km from the south and vary from 1.5 km to 2.2 km for a body at 68 km distance from the south.

Since the profiles in the study area are 2 km apart, differences in computed depth of adjacent profiles for the same anomalies may actually represent lateral variation in depths of the magnetic structures giving rise to the anomalies.

4.3.2 Quantitative Modelling

The Chad Basin, just like the Benue Trough is assumed to be underlain by granite-gneiss and intrusive being the dominant rock types of the Nigerian Basement Complex (Ojo, 1990). Although no magnetic susceptibility data exists for the Chad

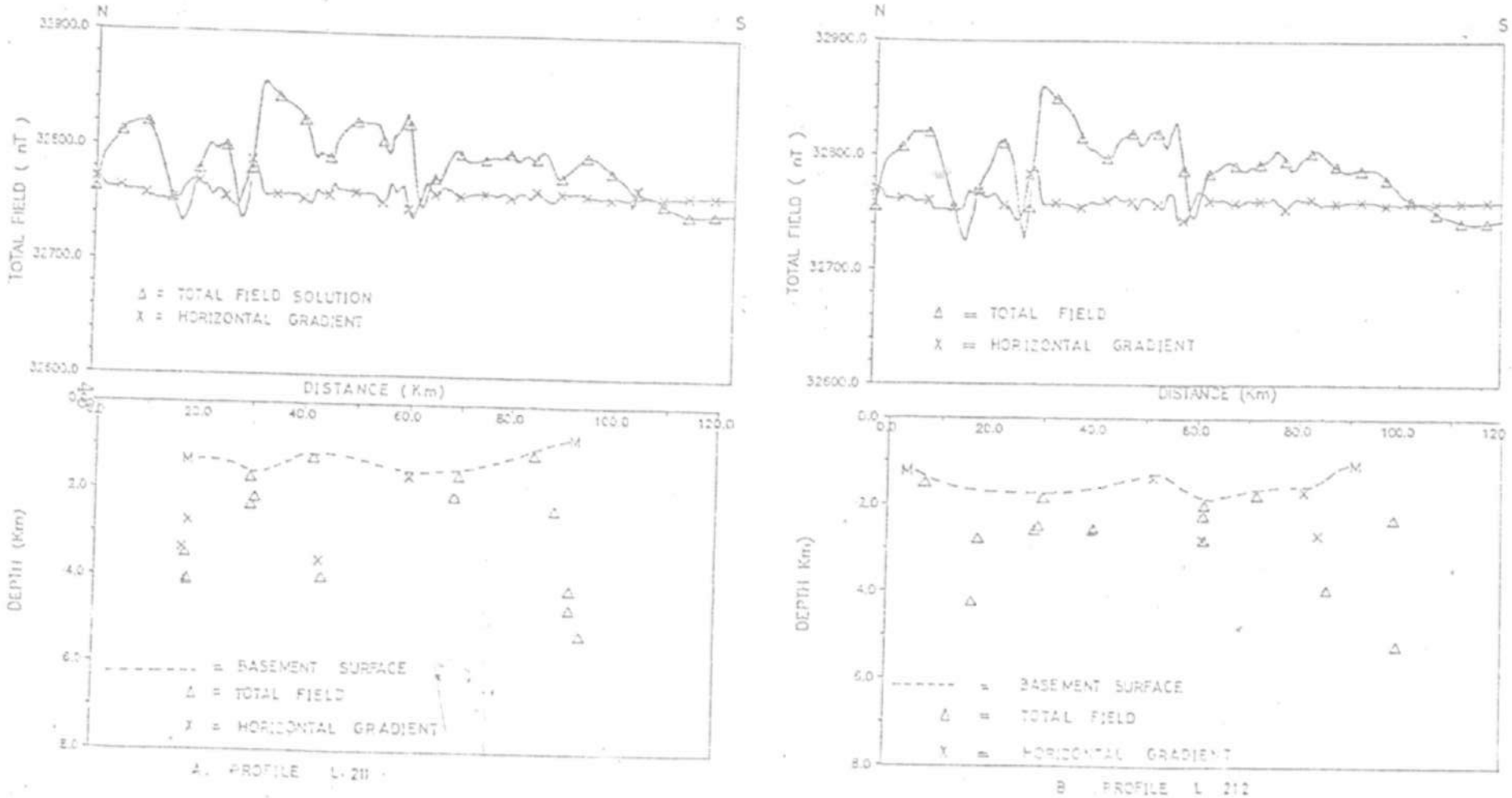


FIG. 4·4 WERNER PROFILES FOR PROFILES L 211 & L 212 .

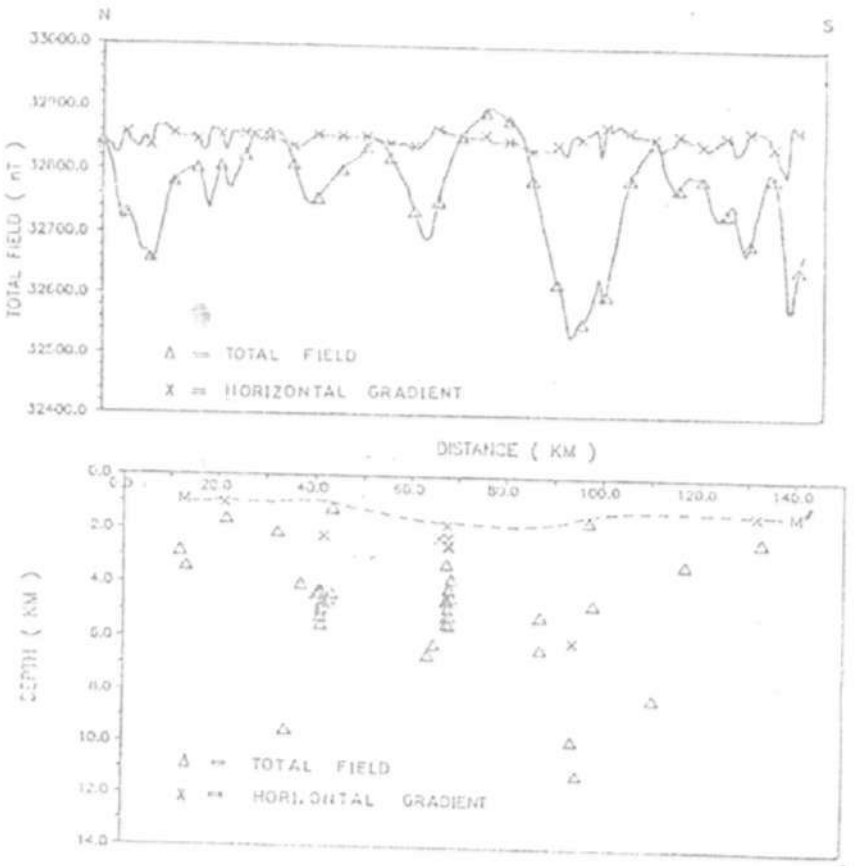


FIG 4·5 WERNER PROFILE FOR PROFILE L 178

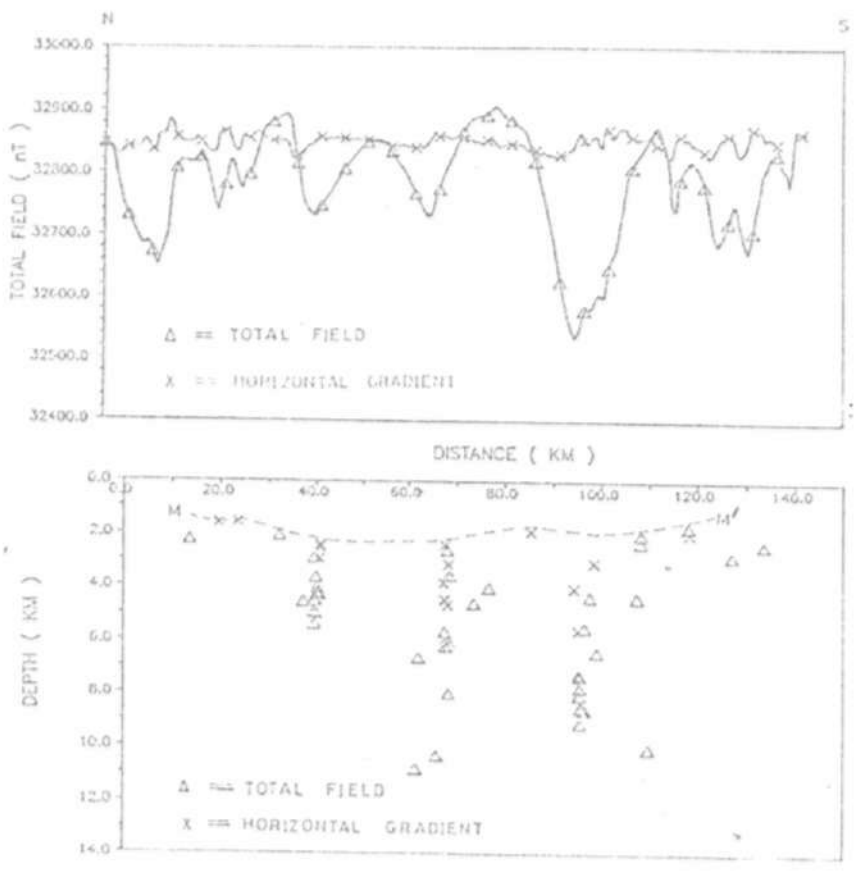


FIG. 4·6 WERNER PROFILE FOR PROFILE L.

Basin region, Ajakaiye (1981) and Ozasuwa et al. (1981) reported ranges of 0.0059 - 0.0097 SI units and 0.15 - 1.030 SI units respectively for granite-gneiss in the neighboring Benue trough to the SW of the Chad Basin.

In this work, three profiles (AA^{1}, BB^{1} and CC^{1}) shown in fig 4.3 were selected for modelling assuming a susceptibility value of 0.0059 SI units for the bedrock. This value lies within the range of susceptibility values obtained by Ajakaiye (1981) for the Benue Trough. In all the models generated for the interpretation, efforts were made to obtain a good fit between the calculated and the observed curves. The detailed description of the final model (interpretation) obtained for each of the profiles is as given below.

Modelling Along Profile AA^{1}

Profile AA^{1} is a short profile 60 km long oriented in NE - SW direction so as to make it cut across the major anomaly in the area at approximately 90^{0}. In the quantitative modelling of Profile AA^{1} (fig 4.8), a susceptibility value of 0.0059 SI units was also used for the bedrock and 0.0092 SI units which was the overall average susceptibility value obtained from the Werner depth solutions was used as the average Susceptibility value of the intrusive body. This susceptibility value was kept constant and the boundaries of the source bodies were allowed to shift positions by changing the body coordinates till a best fit of the observed and calculated curves is obtained. The thickness of the sediments

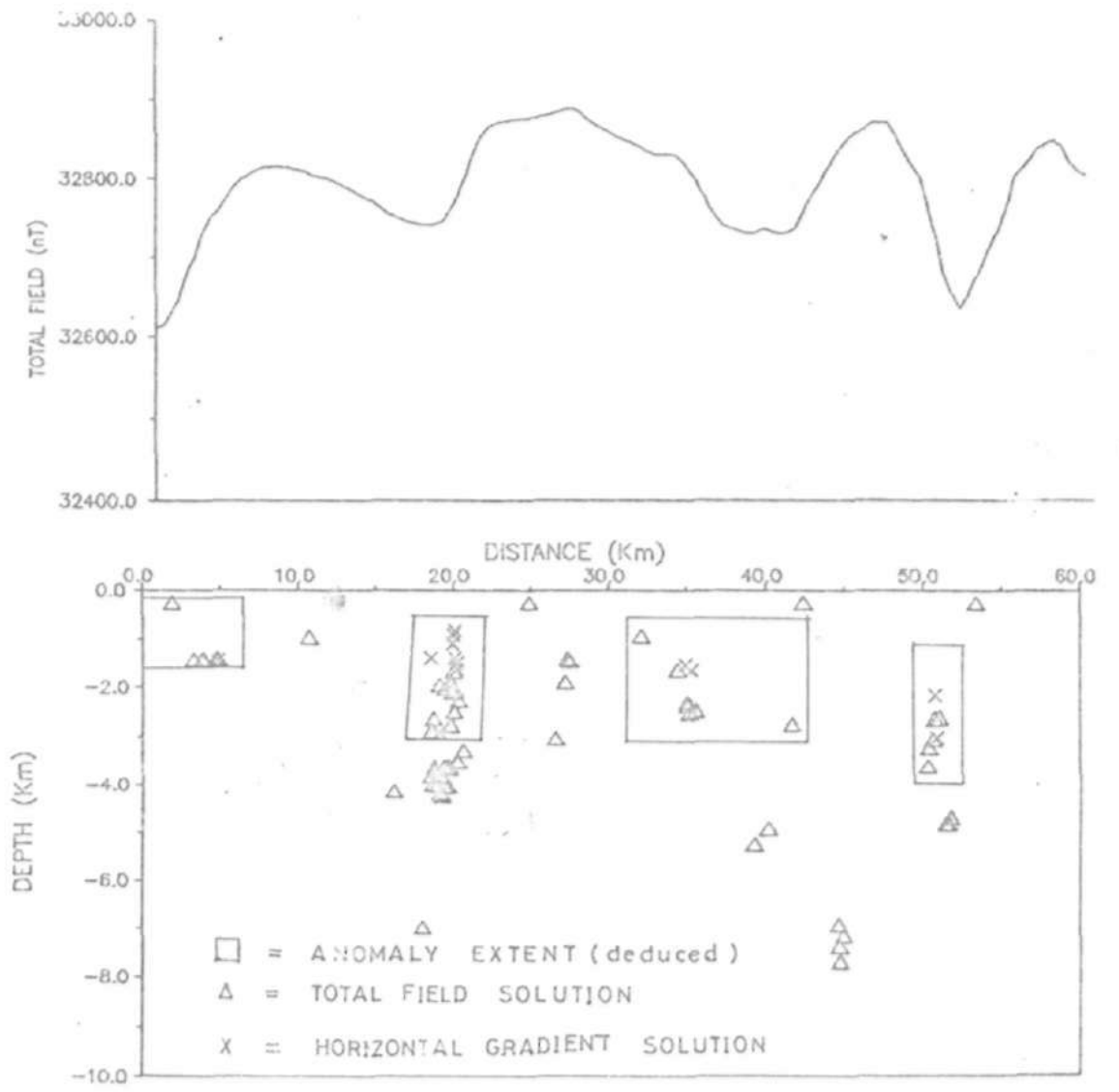


FIG. 4·7 MAGNETIC ANOMALY AND WERNER PLOT FOR PROFILE

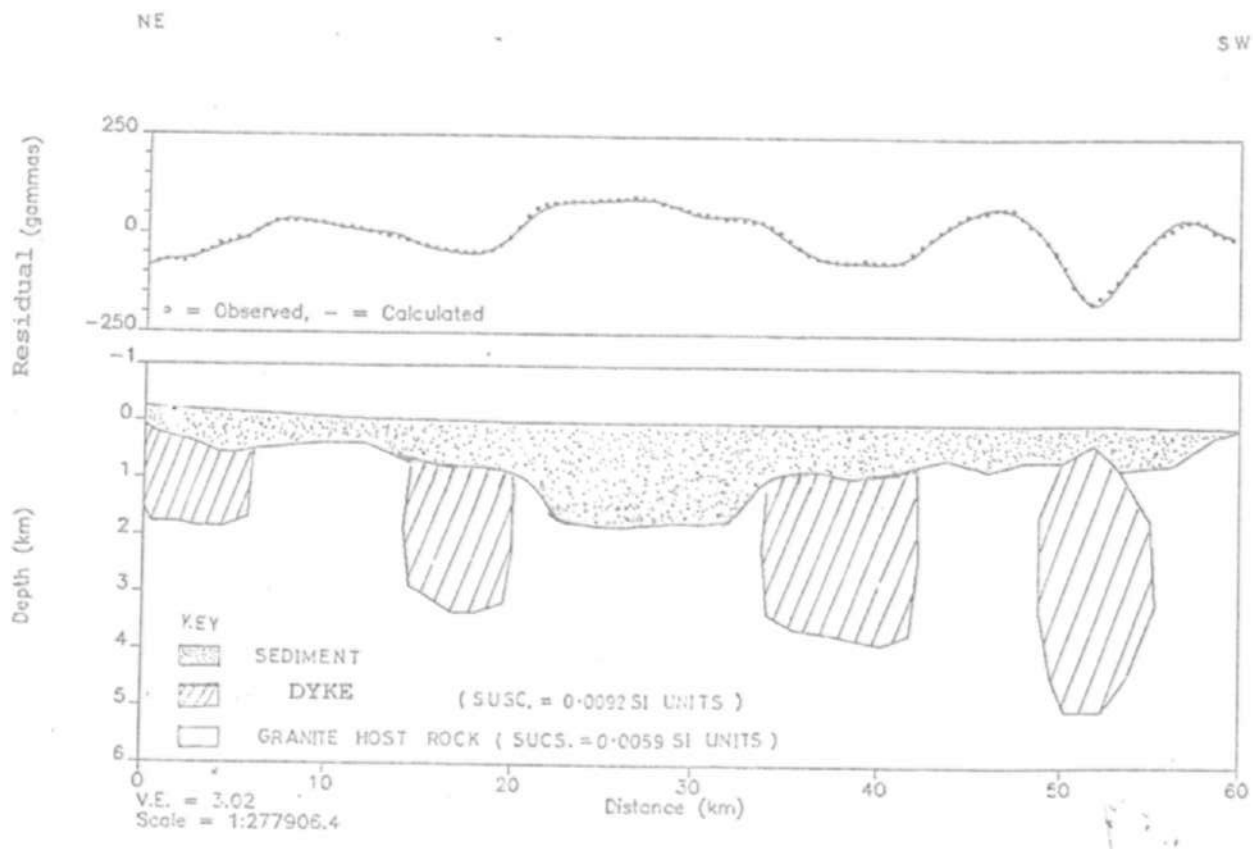


FIG. 4·8 THE MAGNETIC ANOMALY AND INTERPRETED MODEL FOR PROFILE AA'

beneath profile AA^1 was allowed to range from 0.3 km - 0.8 km. The important parameters of the interpreted profile are summarized in table 4.1. The depth values from the Werner profile (fig 4.7) agrees with this result.

TABLE 4.1: Important Parameters of Interpreted Model for Profile AA^1

Body	Position (km)	Susceptibility (SI Units)	Depth – to - Top (km)	Depth – to - Bottom	Width (km)
1	6.0	0.0092	0.3	1.7	5.9
2	20.0	0.0092	0.6	3.3	5.3
3	37.0	0.0092	0.8	3.8	7.9
4	52.0	0.0092	0.5	4.9	6.5

Modelling Along Profile BB^1

This profile is long (140 km), compared to profile AA^1 (60 km). It is an N - S profile cutting across the intrusions at the eastern part of the total field map. In the interpreted model for Profile BB^1 (fig 4.12), five intrusions were observed, a susceptibility value of 0.0072 SI Units which was the overall average obtained from the Werner depth analysis and which also lies within the range of susceptibility values obtained by Ajakaiye (1981) for the neighboring Benue trough was used for these bodies to obtain the best fit to the observed curve. The thickness of sediments within this

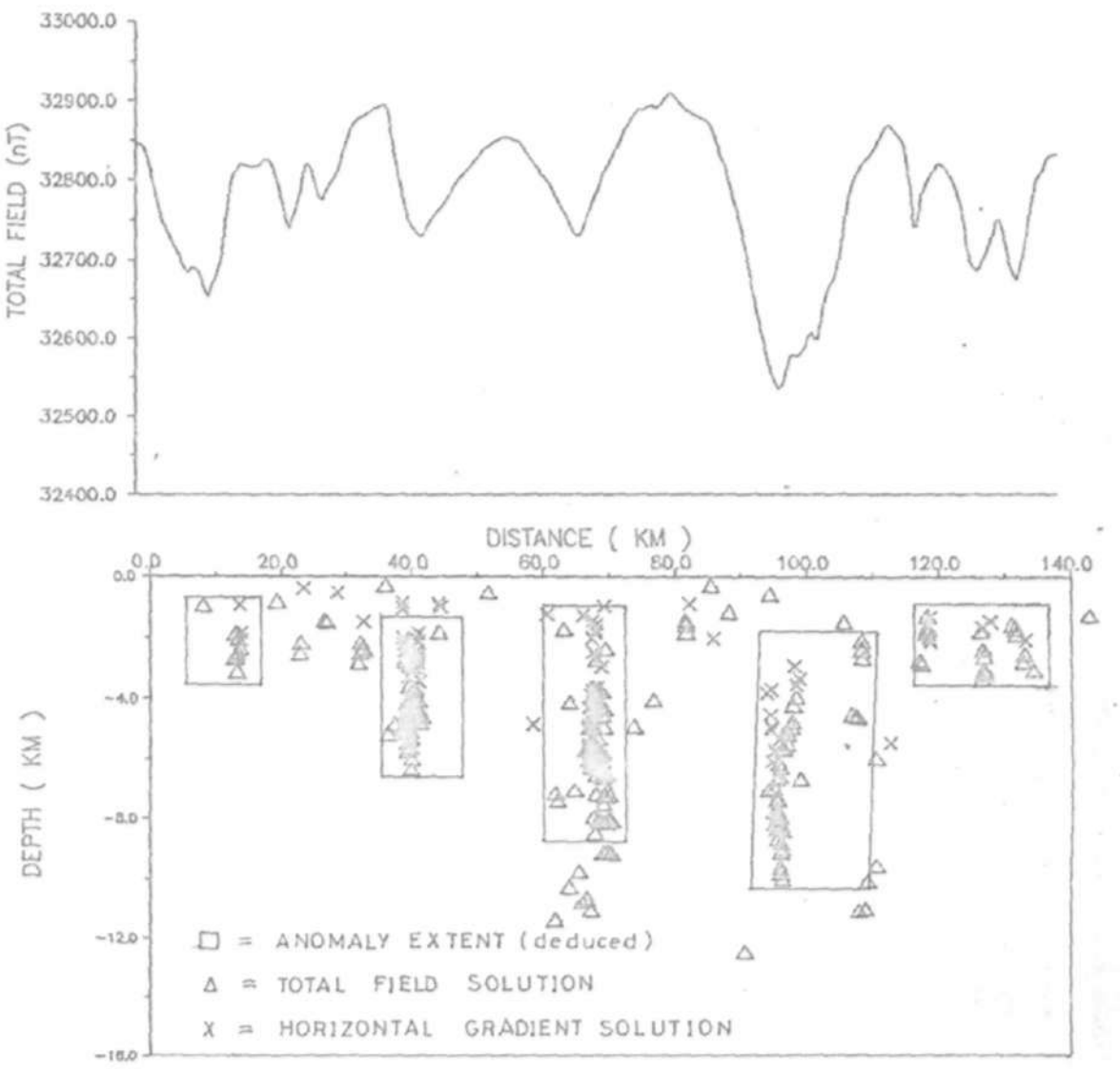


FIG 4.9 MAGNETIC ANOMALY AND WERNER PLOT FOR PROFILE BB'

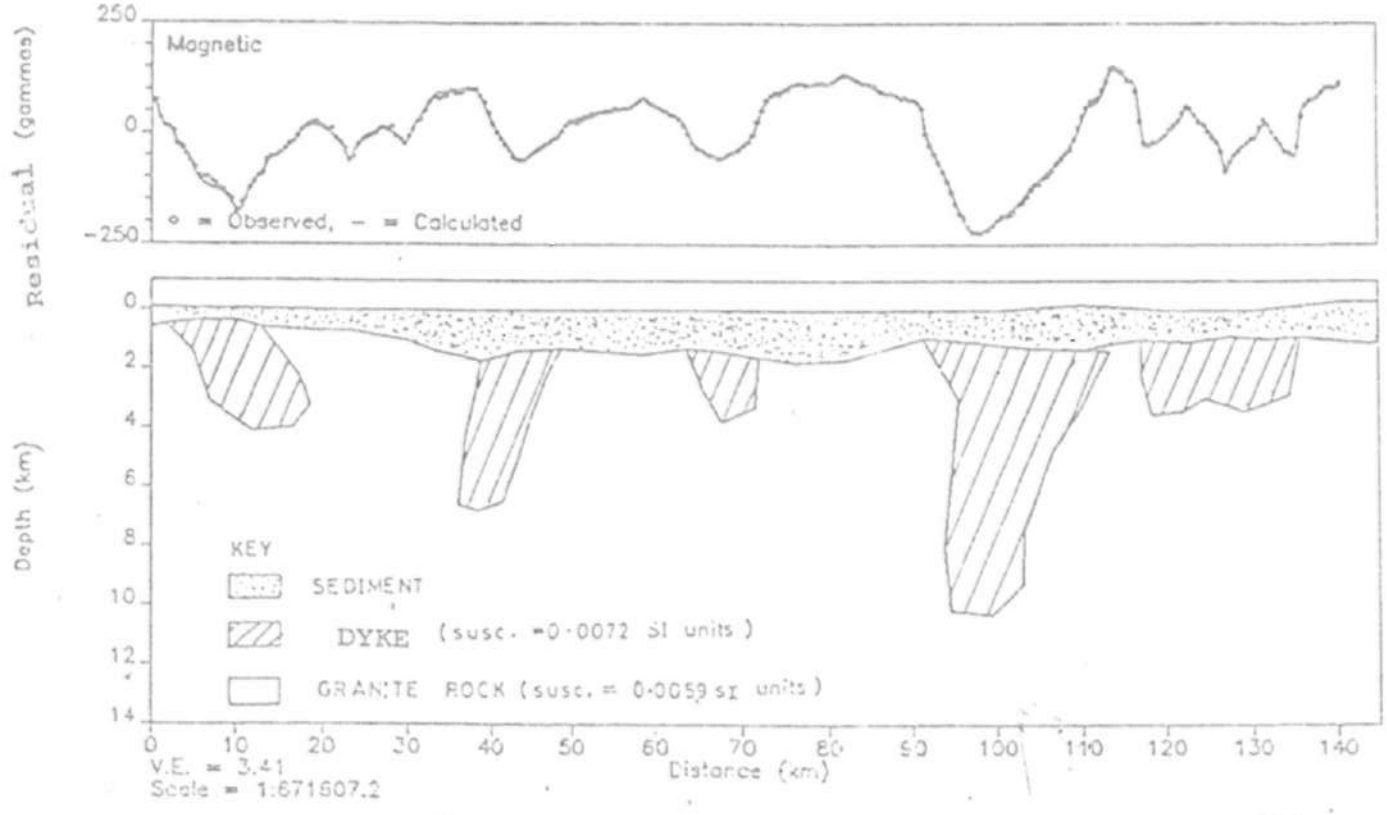


*FIG 4·10 MAGNETIC ANOMALY AND THE INTERPRETED MODEL FOR PROFILE · BB'

profile ranges from 0.4 km - 1.3 km, and the depths to the top and bottom of the various bodies range from 0.4 km - 1.3 km and 3.6 km - 10.2 km respectively as can be seen in Table 4.2. The Werner depth result shown in figure 4.11 agrees with the model result. The divergence of the anomalies towards the surface could be as a result of the steady cooling of the magmatic activity occurring in the host rock.

TABLE 4.2 Important Parameters of Interpreted Model for Profile BB$^{/}$

Body	Position (km)	Susceptibility (SI Units)	Depth – to – Top (km)	Depth – to – Bottom (km)	Width (km)
1	4.1	0.0072	0.4	4.1	13.6
2	6.8	0.0072	1.3	6.6	12.8
3	3.8	0.0072	1.2	3.7	8.7
4	10.8	0.0072	0.9	10.2	22.0
5	2.6	0.0072	0.9	3.6	17.8

Modelling along Profile CC$^{/}$

This profile is moderately long, 120 km. It is a NW - SE profile cutting across the anomaly in the region. The interpreted model for Profile CC$^{/}$ (fig 4.14) has six intrusive bodies, a susceptibility value of 0.0067 SI Units which was the overall average obtained from the Werner analysis was used for these bodies to attain a good fit of the observed

and calculated curves. The thickness of the sediments, which was the depth to the top of the anomalies, ranges from 0.4 km - 1.1 km, and the depth to the bottom of the various anomaly ranges from 1.7 km - 3.7 km (Table 4.3). The equivalent Werner depth result is shown in figure 4.14. The suggestion of the presence of intrusive with high magnetic susceptibilities when compared with the susceptibility of the host rock as revealed by this study may therefore, be the first indication of basic to intermediate rocks and volcanic activity along the chosen profiles. High magnetic susceptibilities are normally found in bodies with mafic to ultramafic composition.

TABLE 4.3: Important Parameters of Interpreted Model for Profile CC'

Body	Position (km)	Susceptibility (SI Units)	Depth – to – Top (km)	Depth –to – Bottom (km)	Width (km)
1	3.5	0.0067	0.4	3.4	10.8
2	2.8	0.0067	0.6	2.8	8.4
3	3.8	0.0067	1.1	3.7	15.8
4	3.6	0.0067	0.7	3.2	11.8
5	1.6	0.0067	0.4	1.7	14.3
6	3.2	0.0067	0.5	2.9	11.8

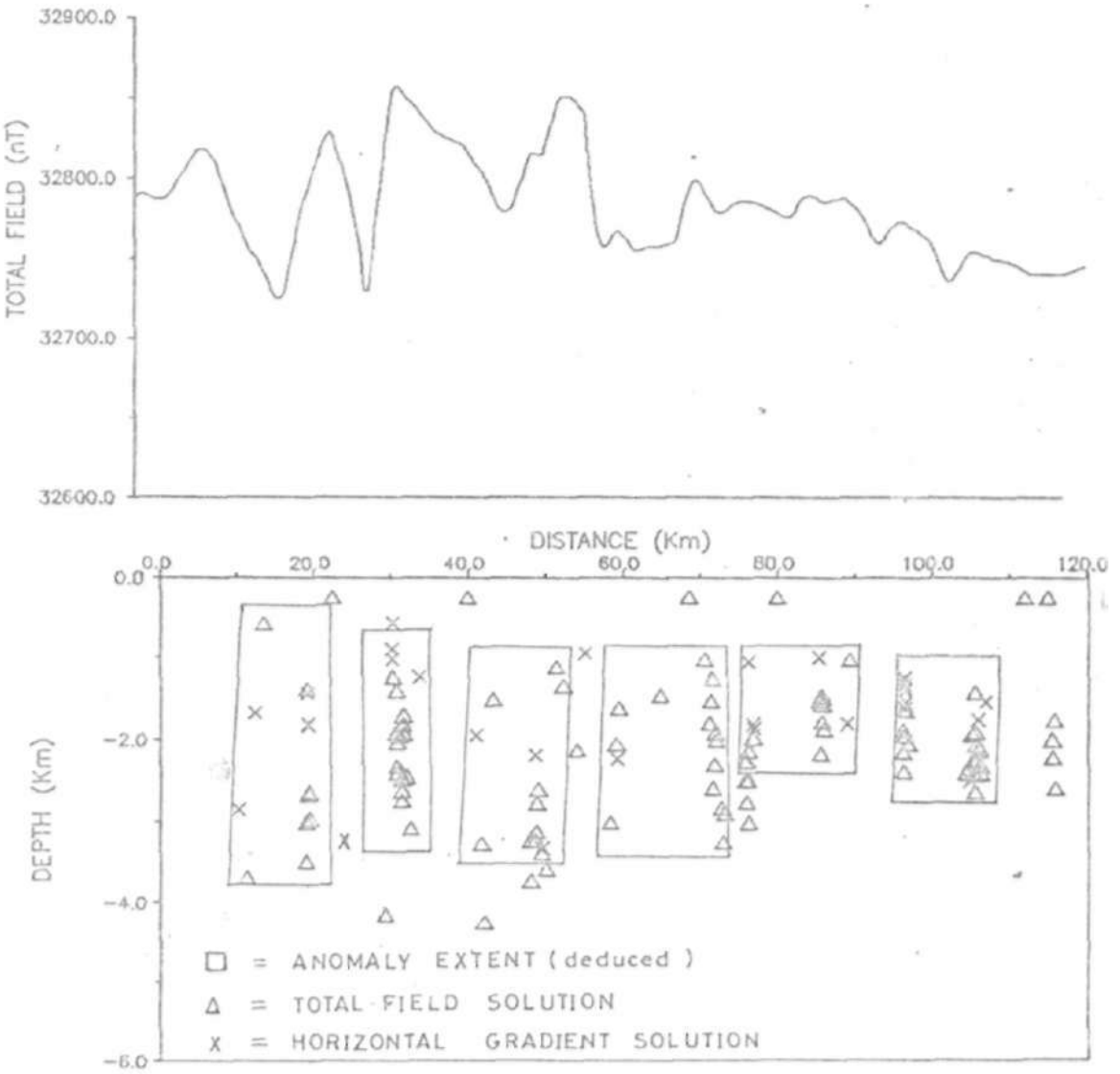


FIG 4.11 MAGNETIC ANOMALY AND THE WERNER PLOT FOR PROFILE CC'

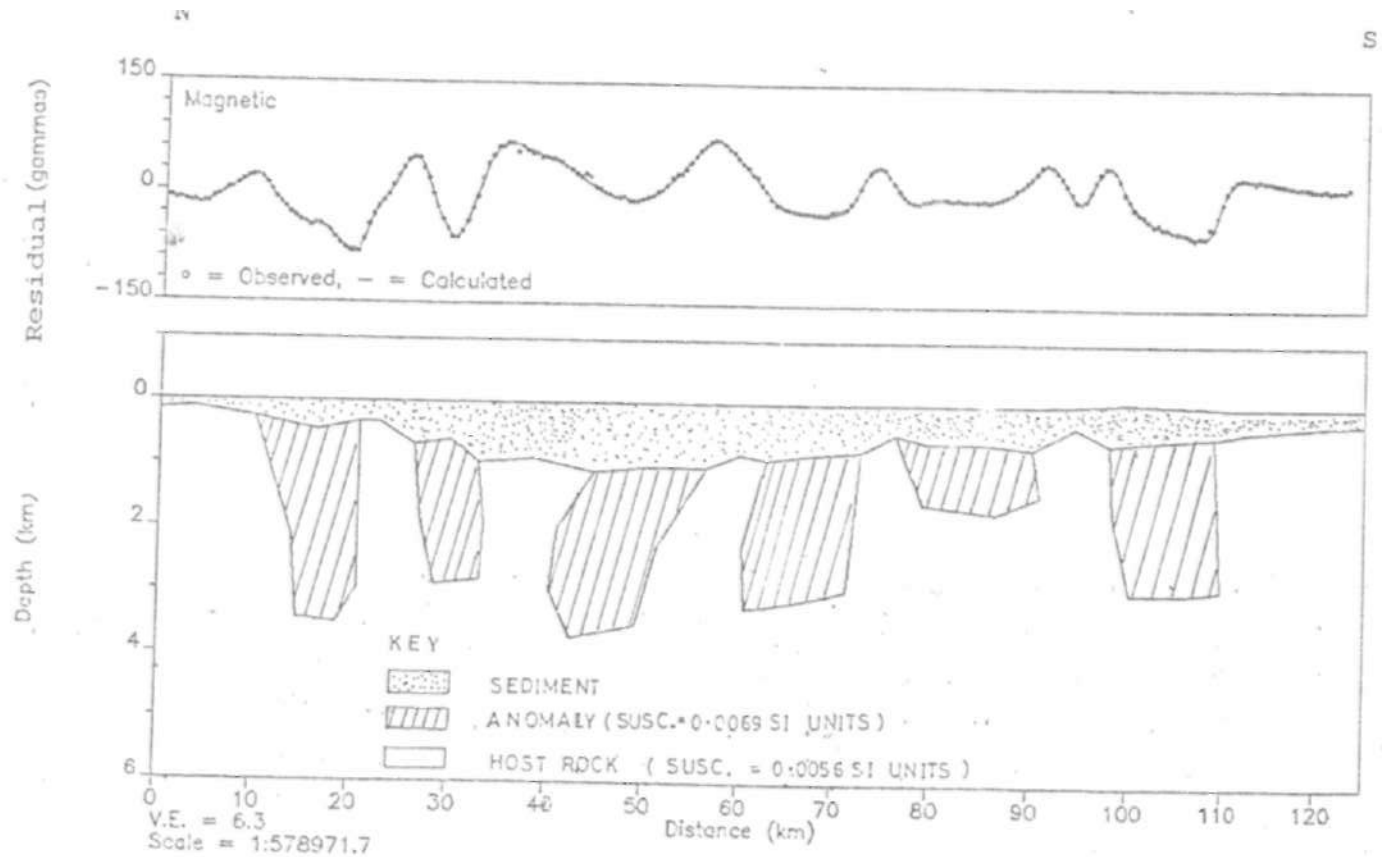


FIG. 4·12 MAGNETIC ANOMALY AND THE INTERPRETED MODEL FOR PROFILE CC'.

4.4 The Depth to the Magnetic Basement Map.

Owing to the fact that the Werner Deconvolution method (Werner, 1953) provides close approximations of depth to the top of the magnetic source and a careful study of the results of all profiles deconvolved in this work, a map giving an idea of the approximate depths to the basement in the study area is produced and this is shown in figure 4.13. The first step taken in preparing the map was to determine the acceptable depth to the top of the intrusions from each profile deconvolved in this work. The input parameters used in the map included the longitude and latitude of each accepted depth (Appendix 1). Figure 4.13 gives the topography of the basement underlying the project area. It also suggests that the thickness of the sediments in the study area vary from 0.3 km to 2.1 km with a general increase in depth from West to East. The basement surface map makes it possible to infer or deduce the presence of structures associated with the basement underlying the project area. Figure 4.14 depicts the contour map of the depth to the basement. The intrusions are almost horizontal with slight orientation in the NE direction. The highest depth to the top of the intrusions corresponding to 2.1 km is seen at the central portion of the map. Shallower depths are obtained in most of the locations except in few areas where the depths extends up to 2 km as seen in the central and NE portions of the map. The depth increases from west and east towards the center of the map.

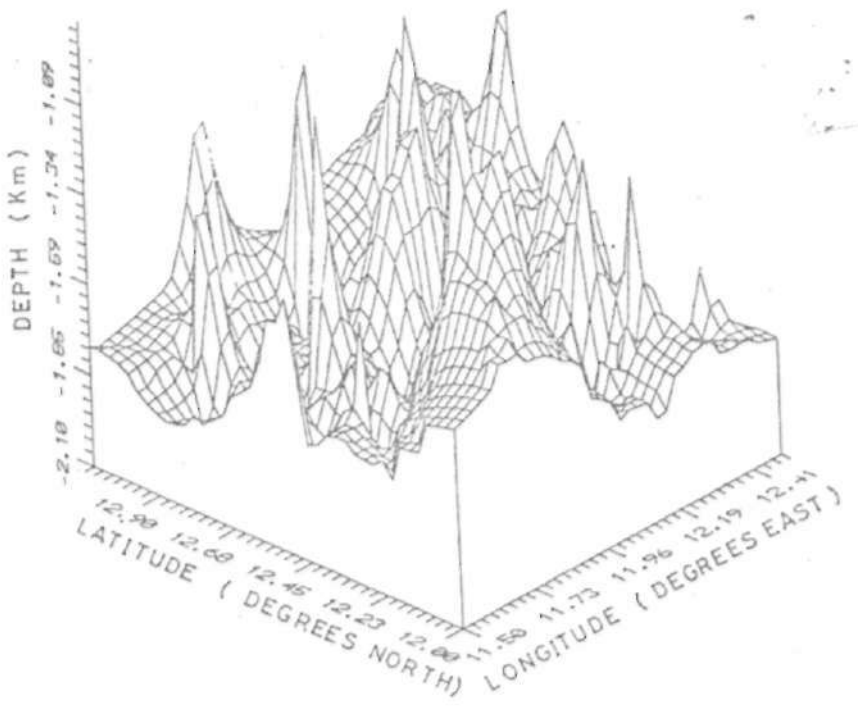


FIG. 4.13 SURFACE MAP OF DEPTH TO THE BASEMENT

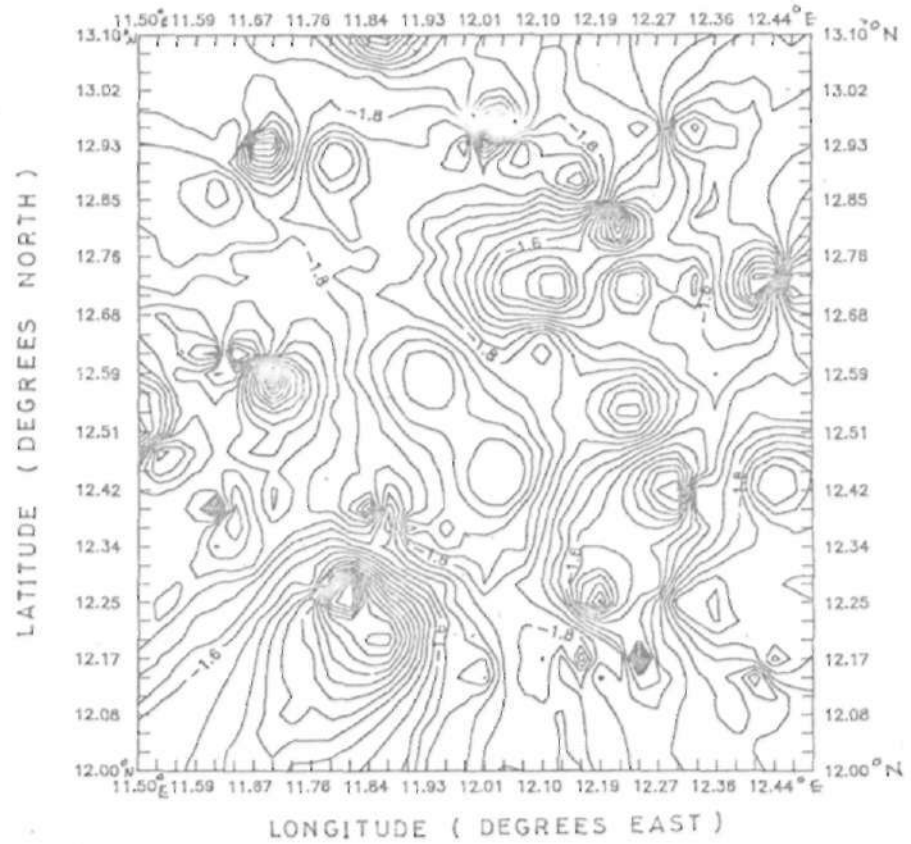


FIG 4.14 Contour Map of Depth to the Basement Contour interval = 0·04Km

CHAPTER FIVE

DISCUSSION AND CONCLUSION

5.1 Discussion of results

The Werner deconvolution results of one profile was correlated with the result obtained from the adjacent profiles to see clearly the extent of any anomaly that spans through more than one profile. The information obtained from the Werner deconvolution results for all the profiles used in this work are as follows: the horizontal location, the depth, the dip, susceptibility value of the causative body and the weighting coefficients of the source body (anomalous body).

5.1.1 Trends of Magnetic Field in the Study Area

Inspection of the total field map (figure 4.1), the residual field map (fig 4.3), and the regional field map (fig 4.2), shows that the magnetic field over the study area has three distinct trends namely; the E - W and the NW – SE trends which are few and the NE - SW trend which is more common. Many of the anomalies in the maps have short wavelengths and small widths suggesting that they are shallow. The anomalies are more or less elliptical in shape suggesting that they are likely to be dikes of basic igneous rocks. The analysis of the total field map shows that the NW - SE trending anomalies are

few while anomalies with NE - SW trend are the most common. The residual field and the regional field maps of the study area also confirm these facts. Although, shallow bodies may effectively mask deeper sources, the Werner deconvolution method is good for providing meaningful interpretations in many cases where magnetic anomalies originate at more than one level.

5.1.2 Types of Intrusions in the Study Area (Based on Susceptibility Values)

We can deduce from figures 4.4 - 4.6 that the observed magnetic contour over the area could best be explained by a combination of variable basement topography and the presence of deep intrabasement intrusive bodies as seen in the model results of figures 4.7, 4.9 and 4.11 respectively, where variation in basement structures and changes in magnetic susceptibility were observed.

The configurations of the anomalies were obtained using GM-SYS modelling procedure. The analyses in tables 4.1 - 4.3 indicate that the depth to the top of intrusions causing the anomalies are at depths lying within 0.3 km - 1.3 km, and the depths to the bottom of the intrusions range from 1.7 km - 10.2 km. With the assumed susceptibility value of the basement being 0.0059 SI Unit, the susceptibility of the intrusions was determined to range from 0.0067 SI Unit - 0.0092 SI Unit, which suggest that it is probably of basic igneous composition. In Telford et al, (1982), The values of basic igneous rock is 0.0092 SI Units.

5.1.3 Thickness of the Basin in the Study Area

The basement surfaces were estimated by correlating the depth to the top of anomaly results obtained from all the fifty-six profiles of the study area. The calculated depth, which varies from 0.3 km - 2.1 km from the interpreted surfaces, was used for compilation of a basement surface map of the area. Werner deconvolution method can be said to be a quick and reliable method of locating the top of intrusions causing the anomalies with desired accuracy. The method shows that although the basement topography varies considerably, depth to the top of the basement along the profiles are generally not greater than 2.1 km. They range between depth of 0.3 km to 2.1 km.

REFERENCES

AJAYI, C.O AND NKEREUWEM (1992). Determining the location of the intra - sediment igneous intrusions and basement structure in the Chungowa Depression, Chad Basin, Nigeria, from aeromagnetic data. A paper presented at the 28th N.M.G.S annual conference, Port - Harcourt.

AJAKAIYE, D.E. (1981): Geophysical investigation in the Benue trough - a review, Earth Evol. Sci. 1:110-125.

AJAKAIYE, D.E. AND BURKE, K. (1973): A Bouguer Gravity Map of Nigeria. Tectonophysics, Vol. 16, pp. 103 - 115.

AJAKAIYE, D. E AND VERHEIJEN, P (1983): An Analysis of a possible episodic plume trace in West Africa. Geophy. Res. Let. 10, 424 – 427

ASGA -UNESCO. (1973): Carte Geologique de l'Afrique. 1:5,000,000. Feuille No 2. Paris.

AVBOVBO, A. A., AYOOLA, E. O. AND OSAHON, G. A. (1986): Depositional and structural styles in Chad Basin of north -Eastern Nigeria. AAPG Bull. Vol., 70,pp.1787 - 1798.

BARBER, W. (1965): Pressure water in the Chad formation of Bornu and Dikwa Emirates, north - eastern Nigeria. Bull. Geol. Surv. Nigeria, vol., 35, 138pp.

BHATTACHARYA, B.K. (1971): An automated method of compilation and mapping of high - resolution aeromagnetic data. Geophysics, vol., 36, pp. 695 - 716.

BHATTACHARYA, B.K. AND LUE, L.K (1975): Analysis of magnetic anomalies over yellow stone National park: Mapping of Curie point isothermal surface for Geothermal reconnaissance. *Journal of Geophysical research.* Vol. 80(32), pp. 4461 - 4465.

BINKS, R. M. AND FAIRHEAD, J. D (1992): A plate tectonic setting for the Mesozoic rifts of West and Central Africa. Tectonophysics, 213, 141 - 151.

BURKE, K. (1976): The Chad basin: An active intra - Continental basin. Tectonophysics, vol.36 pp. 197 - 206.

CARTER, J. D., BARBER, W., and Jones, G. P. (1963): The geology of parts of Adamawa, Bauchi and Bornu provinces in north eastern Nigeria. Bull. Geol. Surv. Nigeria, vol.30, 109pp.

CRATCHLEY, C.R. (1960): Geophysical survey of the southwestern part of the Chad Basin. Paper presented at CCTA Conference on "Geology", Kaduna, Nigeria, February 1960 (Unpubl.)

DOBRIN, M.B. (1982): Introduction to Geophysical prospecting: 3rd edition: Mc Graw-Hill Book Co., 630p.

FRANKS, S AND NAIRN, A. E. M. (1973): The equatorial marginal basins of West Africa. In: NAIRN, A. AND STEHLI, F. (Eds) - The ocean basins and margins, vol., 1 pp301 - 350. The South - Atlantic -Plenum Press.

FURON, R. (1963): Geology of Africa. Oliver and Boyd Ltd, Edinburgh. London, 377pp.

GAY, S.P, Jr. (1963): Standard Curves for Interpolation of magnetic Anomalies over long Tabular Bodies "Mining Geophysics", vol., 2, pp. 512 - 548, Society of Exploration Geophysicists, Tulsa, Okla.

GENIK, G.J. (1992): Regional framework, structural and petroleum aspects of rift basins in Niger, Chad and Central African Republic (C.A.R). Tectonophysics, 213, 169 - 185.

GENIK, G. J. (1993): Petroleum Geology of Cretaceous - Tertiary rift basins in Niger, Chad and Central African Republic. AAPG Bull.vol.77 (8), pp1405 - 1434

HARTMAN, R. R., TESKY, D. J., & FRIEDBERG J.L. (1971): A system for rapid digital aeromagnetic interpretation: Geophysics, vol., 36,pp.891 -918.

HARTLEY, R. W. AND ALLEN, P. A. (1994): Interior Cratonic basins of Africa: Relation to continental break - up and role of mantle convection. Basin Research vol, 6 pp. 95 - 113.

JAIN, S. (1976): An automatic models: Geophysics, in the determination of regional fields by polynomial fitting: a simple solution, Geophysics, vol., 36 pp.531 - 541

KANGKOLO, R. AND OJO, S.B. (1994): Shortcomings in the determination of regional fields by polynomial fitting: A simple solution, Geophysics vol., 36,pp 205 - 212.

KU, C.C AND SHARP, J.A. (1983): Werner deconvolution for automated magnetic interpretation and its refinement using marquardt's inverse modelling, Geophysics, vol., 48 (6). Pp. 754 - 774.

MATHEIS, G (1976): Short review of the geology of the Chad Basin in Nigeria. Geology of Nigeria. Kogbe, C. A. (Edit.), pp 289 - 294.

ODUSINA, A. A., MUBARAK, S. O., BEKA, F. T. AND NWANGWU, U (1983): Geology and petroleum potential of the Nigerian Sector of the Chad Basin. Research Bulletin, vol. iii ,Exploration Research Section (R & D), Project No. ER/RD/43, N.N.P.C Port-Harcourt, Nigeria. 47p.

OJO, S.B.(1990): Origin of a major aeromagnetic anomaly in the Middle Niger Basin,Nigeria. Tectonophysics, 185, 153 - 162.

OFOEGBU, C. O. (1985). (Ed.) - The Trough: structure and evolution. Friedr.Vieweg & Sohn Verlagesells chaft MbH, Brunch weigh, 287 - 320.

OSAZUWA, I. B, AJAKAIYE, D.E and VERHEIJEN, R.J.T (1981): Analysis of the structure of part of the Benue rift valley on the basis of new geophysical data. Earth Evol. Sci., 1: 126 - 135.

OTI, M. N. (1990): Lower Turonian Carbonates on the Zambuk Ridge, S.E Chad Basin: The Ashaka limestone. In: OFOEGBU, C.O. (1985). (Ed.) - The Trough: structure and evolution. Friedr.Vieweg & Sohn Verlagesells chaft MbH, Brunch weigh, 287 - 320.

PETTERS, S. W. (1981): Stratigraphy of Chad and Ilullemmeden Basin. Eclogue geol. Helv, Vol., 74 (1), pp 139 - 159.

POPOFF, M., WIEDMANN, J & DE KLASZ, I (1986): The upper Cretaceous Gongila and Pindiga formations, northern Nigeria: Subdivisions, age, stratigraphic correlations and paleo - geographic implications. Eclogae geol. Helv. vol., 79 (2), pp 343 - 363.

RASMUSSEN, R., & PEDERSEN, L.B. (1979): End corrections in potential field modelling: Geophysical prospecting, vol., 27, pp. 749 - 760.

TALWANI, M., & HEIRTZLER, J.R. (1964): Computation of magnetic anomalies caused by two - dimensional bodies of arbitrary shape, in parks, G.A. Ed., computers in the mineral industries, part 1: Stanford University publication Geological Sciences, vol., 9, pp. 464 - 480.

TALWANI, M., WORSEL, J.L., & LANDISMAN, M., (1959), Rapid gravity computations for two dimensional bodies with application to the mendocino submarine fracture Zone: J.Geophys. Res., vol., 64. pp 49 - 59.

TELFORD, W.M., Geldart, L.P., Sheriff, R.E. and keys, D.A. (1982): Applied Geophysics, Cambridge University Press, and Cambridge.

TOKARSKY, A. (1973). " Geological possibilities for Chad oil in Nigeria", occasional paper No. 3, Department of Geology, Ahmadu Bello University, Zaria, Nigeria.

VACQUIRE, V., STENLAND, N.C., HENEDERSON, R.G. and ZIETZ, I., (1951): Interpretation of Aeromagnetic maps, Geol. Soc. Mem. Vol., 47. 151pp.

WERNER. S., (1953): Interpretation of magnetic anomalies at sheet - like bodies: Sveriges Geol. Undersok. Ser. C. Arsbok. Vol., 43 (6).

WHITEMAN, A. (1982): NIGERIA; Its Petroleum geology, resources and potential. Graham and Trotman Publ. London. 166p

WON, I. J. & BEVIES, M. (1987): Computing the gravitational and magnetic anomalies due to a polygon: Algorithms and Fortran subroutines: Geophysics, vol., 52, pp 232 - 238.

WRIGHT, J.B., HASTINGS, D.A., JONES, W.B.& WILLIAMS, H.R. (1985): Geology and mineral Resources of West Africa. George Allen and Unwin, London. 171pp.

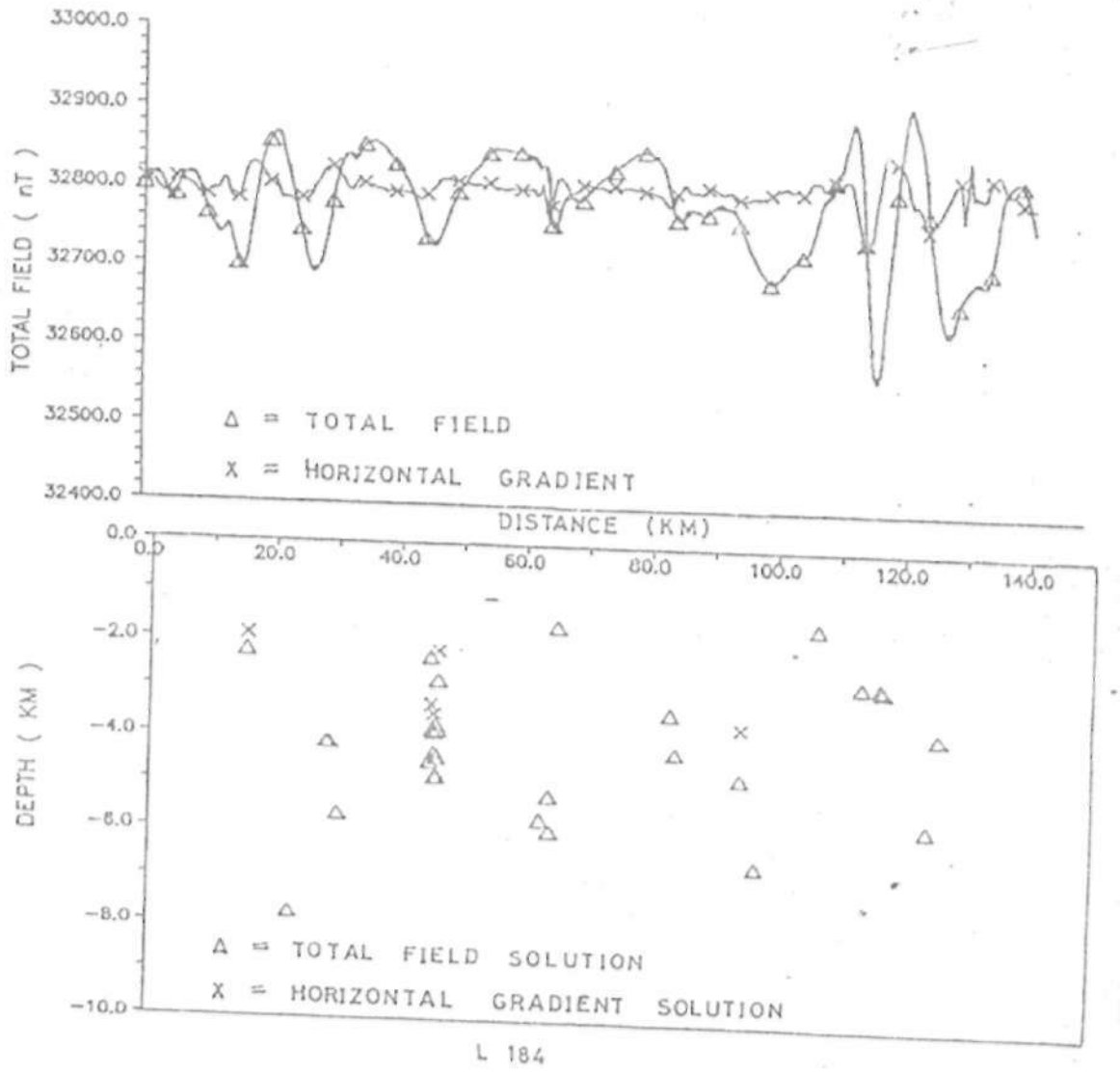
YUSUF, L (1990): Werner Deconvolution and Interpretation of Aeromagnetic data over Parts of the Upper Benue Trough, Nigeria. Unpublished M.Sc thesis A.B.U Zaria.

APPENDIX

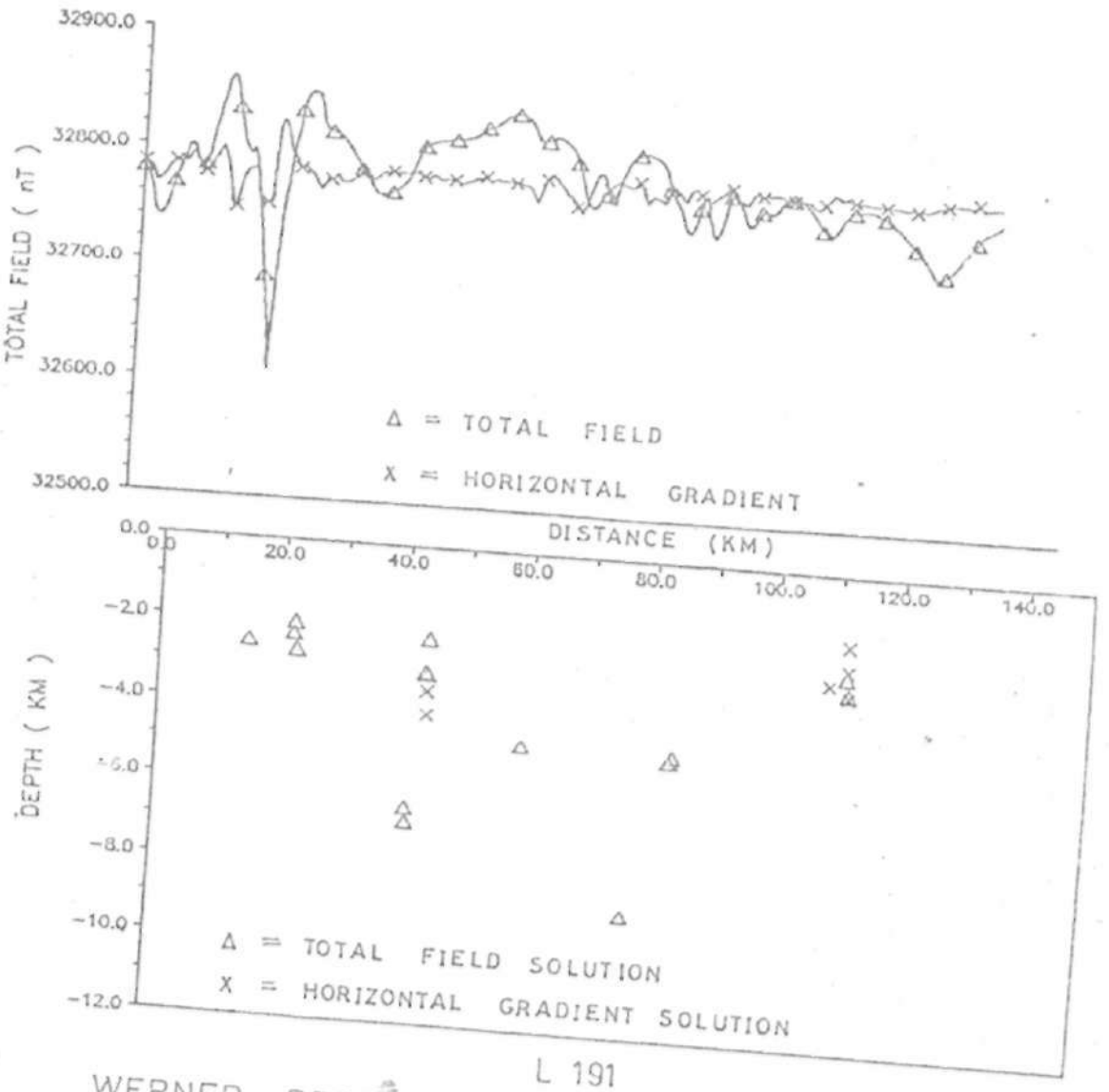
No.	Title	Page
1.	Depths to the top of intrusions	76
2.	Werner profile for profile L 184	78
3.	Werner profile for profile L 191	79
4.	Werner profile for profile L 201	80
5.	Werner profiles for profiles L 187 and L 188	81
6.	Werner profiles for profiles L 182 and L 183	82
7.	Werner profiles for profiles L 189 and L 190	83
8.	Werner profiles for profiles L180 and L 181	84
9.	Werner profiles for profiles L 194 and L 195	85
10.	Werner profiles for profiles L192 and L 193	86
11.	Werner profiles for profiles L196 and L 197	87
12.	Werner profiles for profiles L198 and L 199	88
13.	Werner profiles for profiles L 202 and L 203	89
14.	Werner profiles for profiles L 210 and L 211	90

Flight lines	Longitude (Degree)	Latitude (Degree)	Depth (km)
173	11.51	12.50	1.3
173	11.51	12.50	1.4
174	11.53	12.47	2.0
175	11.55	12.48	1.9
175	11.55	12.86	1.9
176	11.57	12.59	1.8
177	11.59	12.38	1.0
177	11.59	12.62	1.6
178	11.61	12.38	1.0
178	11.61	12.62	1.5
179	11.62	12.36	2.1
179	11.62	12.61	2.1
179	11.62	12.86	2.0
180	11.64	12.62	2.1
181	11.66	12.41	2.0
181	11.66	12.61	1.8
181	11.68	12.59	0.8
182	11.68	12.62	2.1
182	11.68	12.93	1.2
183	11.69	12.41	1.2
183	11.69	12.59	0.8
184	11.71	12.41	2.0
185	11.73	12.41	1.8
186	11.75	12.41	1.8
187	11.77	13.01	1.8
188	11.79	12.91	2.1
189	11.80	12.27	0.6
190	11.82	12.47	1.8
191	11.84	12.40	2.1
191	11.84	13.02	1.8
192	11.86	12.20	1.0
192	11.86	12.40	1.5
192	11.86	13.10	1.5
193	11.88	12.37	1.5
194	11.90	12.37	2.0
195	11.91	12.58	2.0
196	11.93	12.59	2.1
197	11.95	12.36	2.0
197	11.95	12.93	1.8
198	11.97	12.93	2.1
199	11.99	12.93	2.0
200	12.01	12.15	1.5
201	12.03	12.16	1.5
201	12.03	12.44	2.1
201	12.03	12.95	0.8
202	12.05	12.16	1.8
203	12.05	12.92	2.0
203A	12.07	12.16	1.6
204	12.08	12.16	2.0

Flight lines	Longitude (Degree)	Latitude (Degree)	Depth (km)
205	12.10	12.63	1.9
206	12.11	12.16	2.0
206A	12.12	12.16	2.0
207	12.14	12.18	1.9
207	12.18	12.15	1.6
210	12.20	12.86	1.8
211	12.21	12.16	1.8
212	12.23	12.54	2.0
213	12.25	12.17	1.2
214	12.27	12.18	1.8
215	12.29	12.43	1.2
216	12.31	12.26	2.0
217	12.33	12.41	2.0
218	12.35	12.24	2.0
219	12.36	12.27	2.1
220	12.38	12.27	1.8
221	12.40	12.11	1.8
222	12.42	12.13	1.5
223	12.44	12.16	2.0
223	12.44	12.43	2.1
223	12.44	12.74	2.0
224	12.46	12.72	2.0
225	12.48	12.72	1.8
226	12.49	12.74	1.8

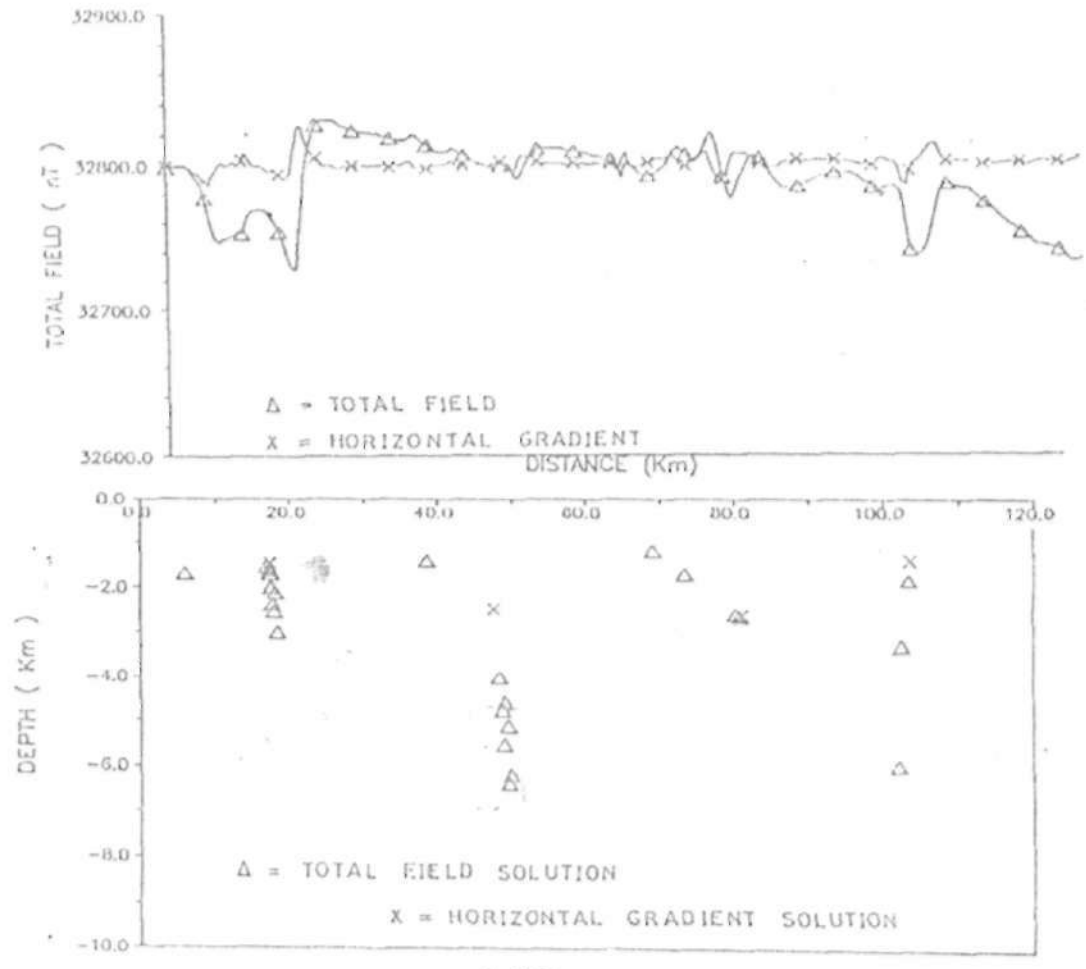


WERNER PROFILES FOR PROFILE L 184



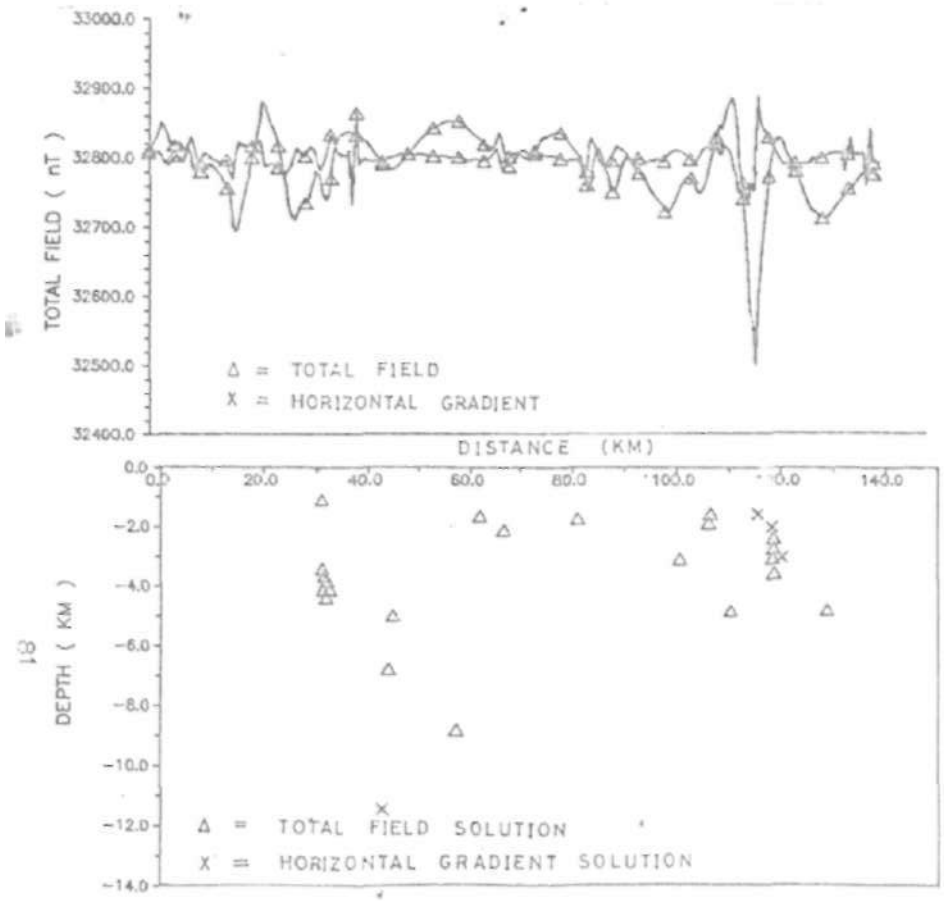
L 191

WERNER PROFILE FOR PROFILE L 191

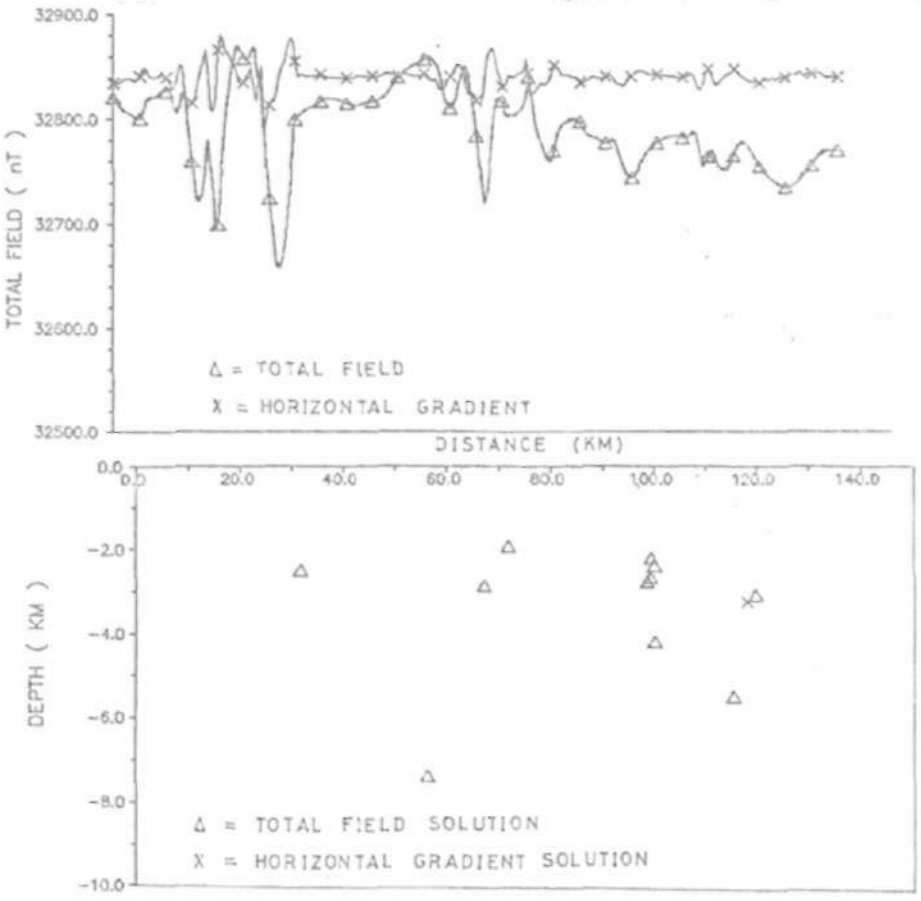


L 201

WERNER PROFILE FOR PROFILE L 201

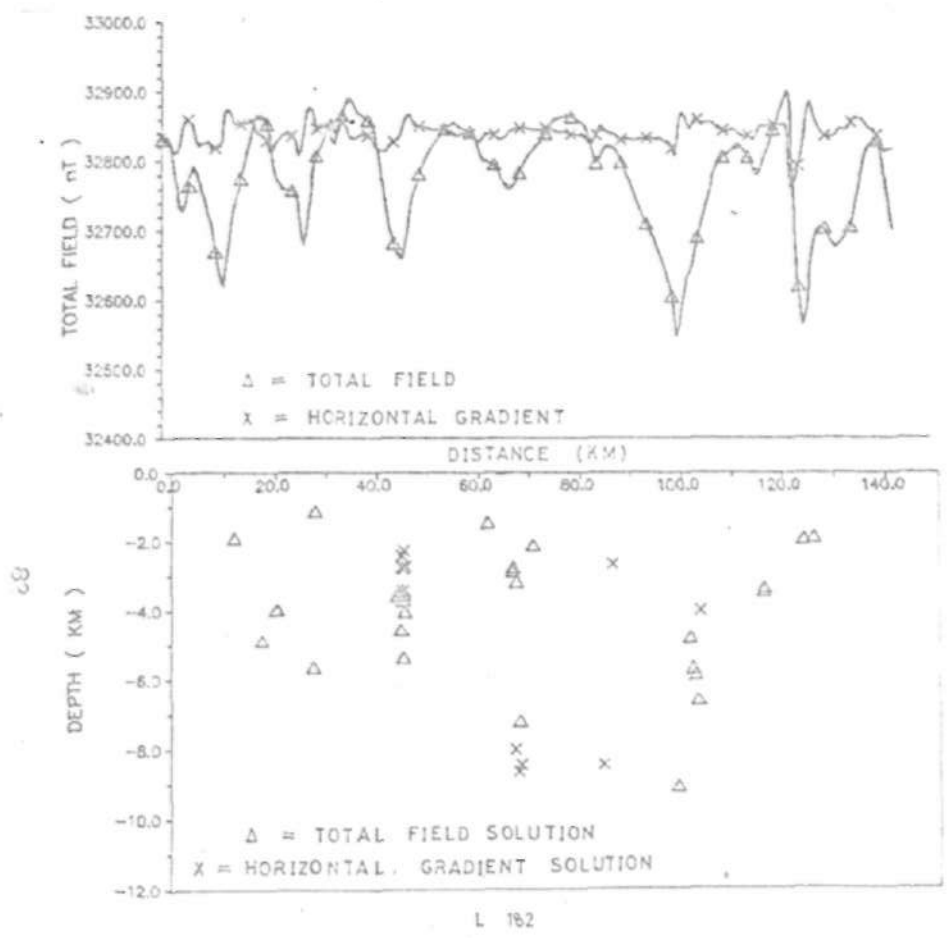


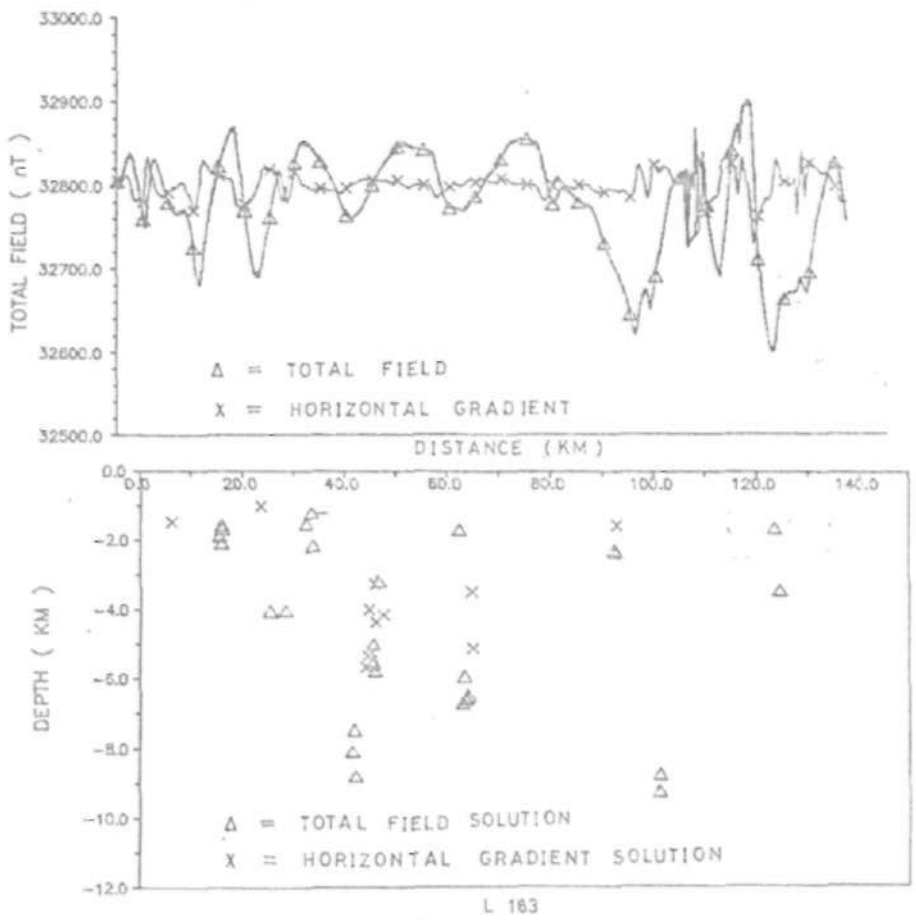
L 187



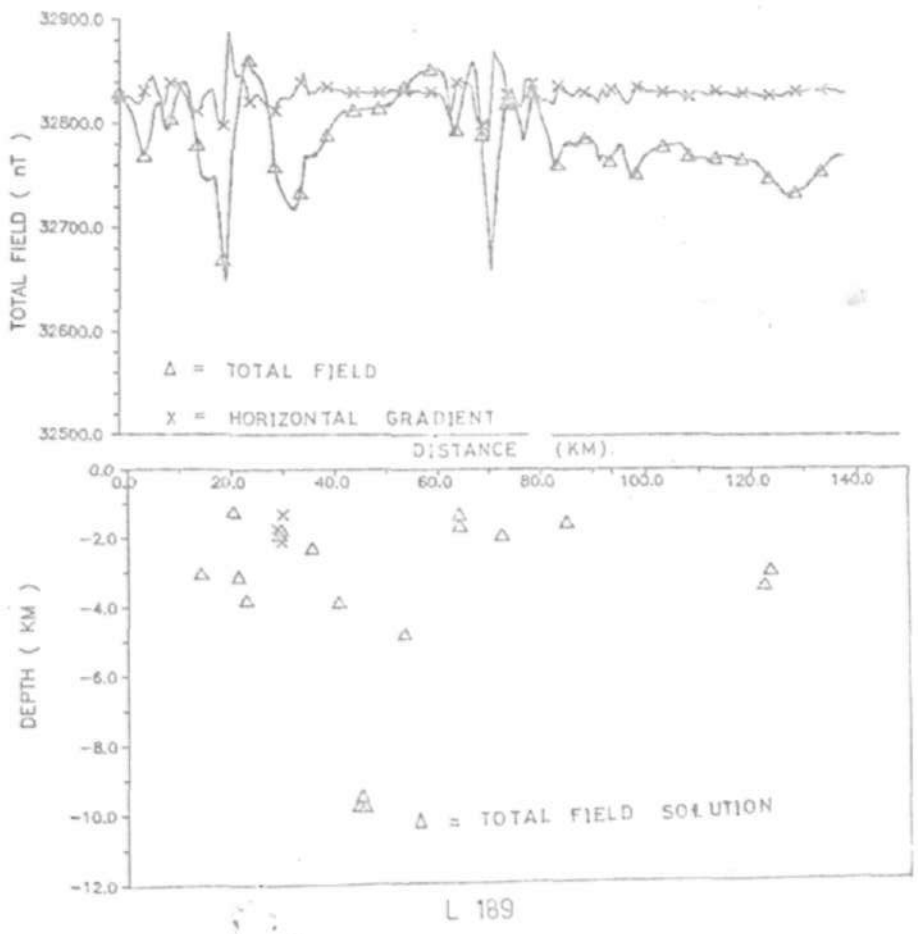
L 188

WERNER PROFILES. FOR PROFILES L 187 & L 188

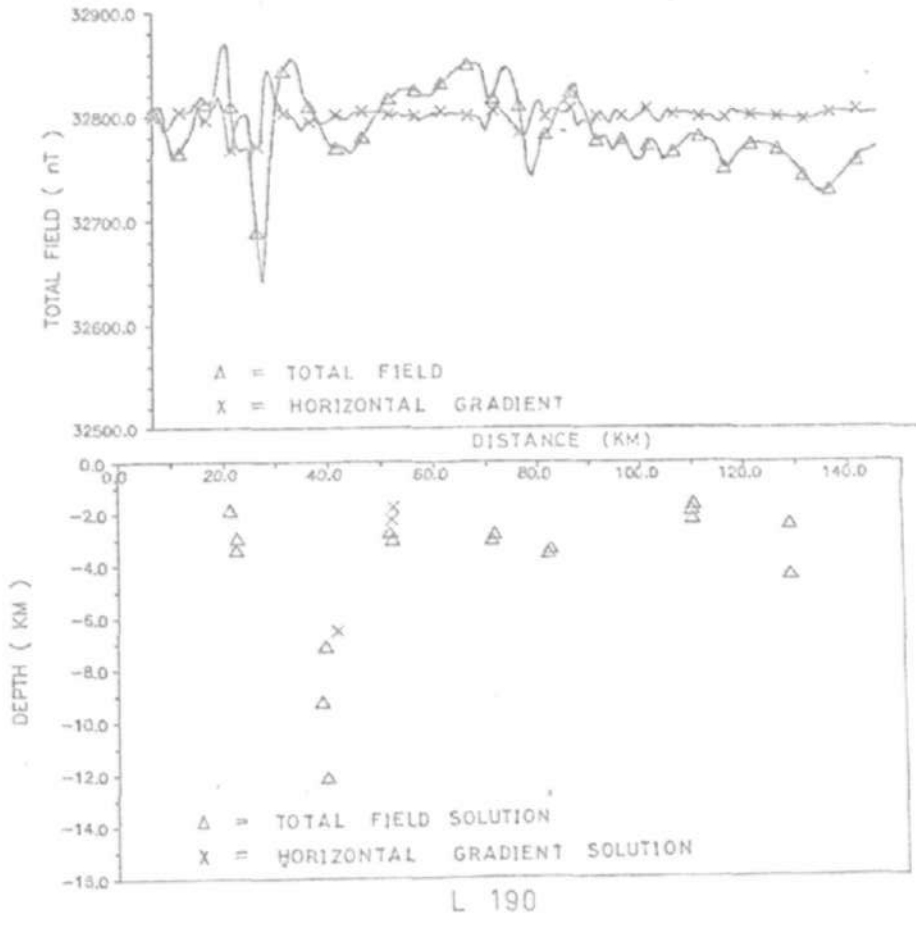




WERNER PROFILES FOR PROFILES L 182 & L 183

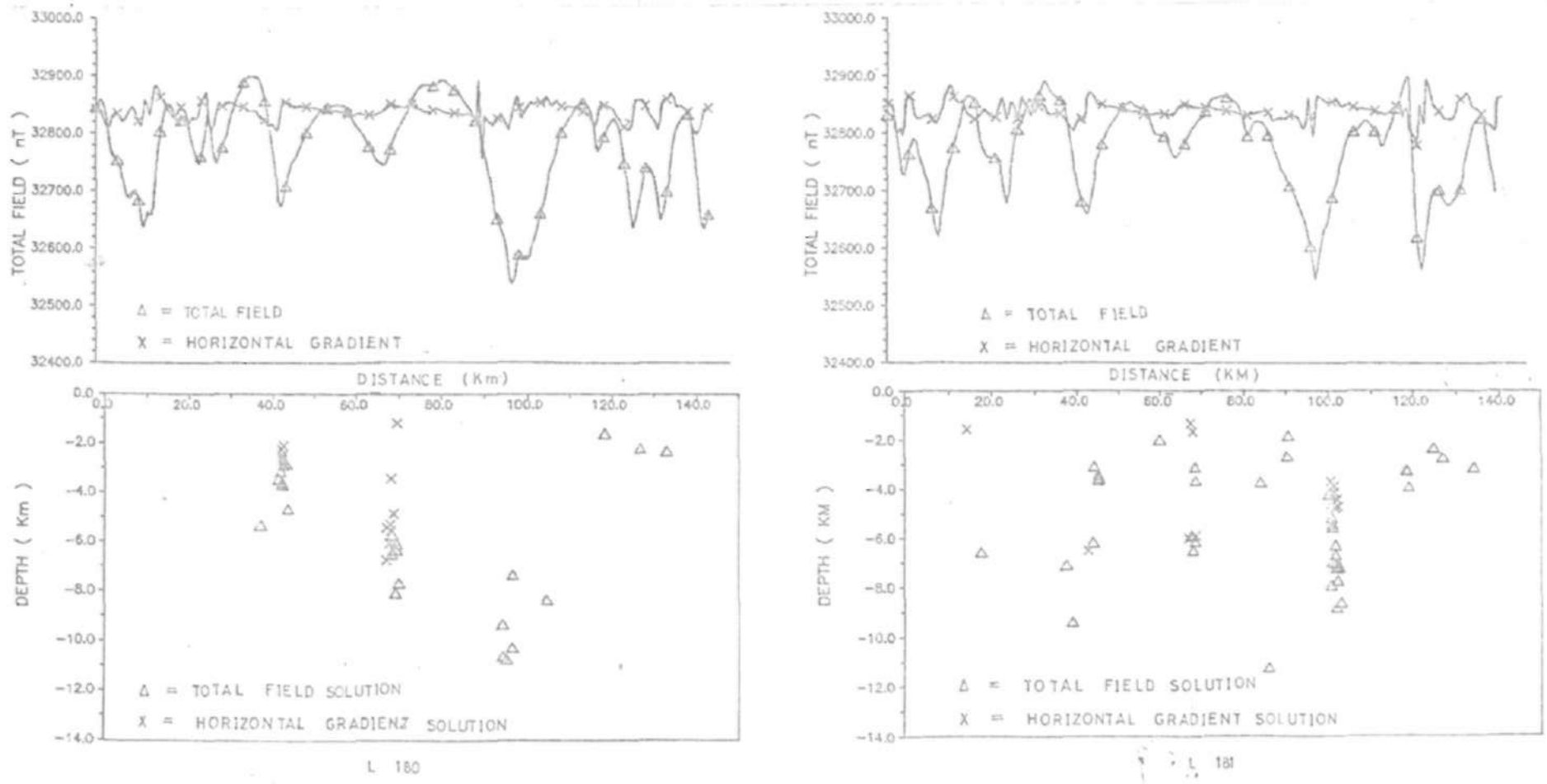


L 189

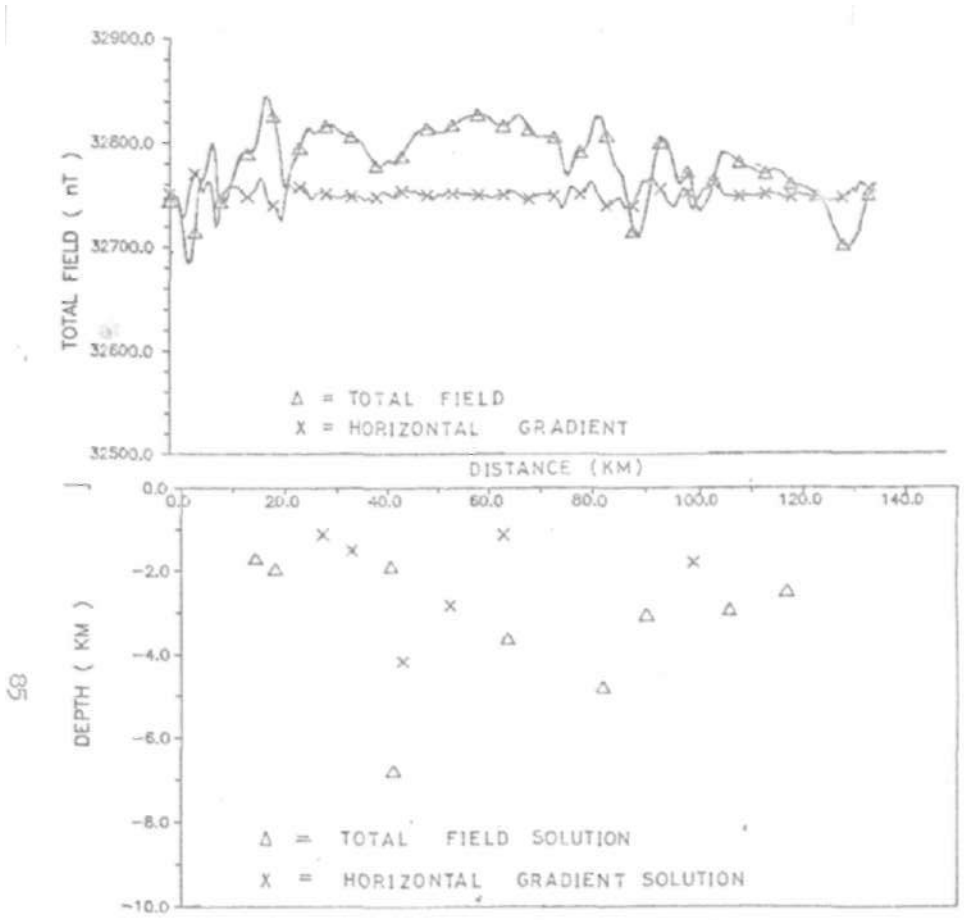


L 190

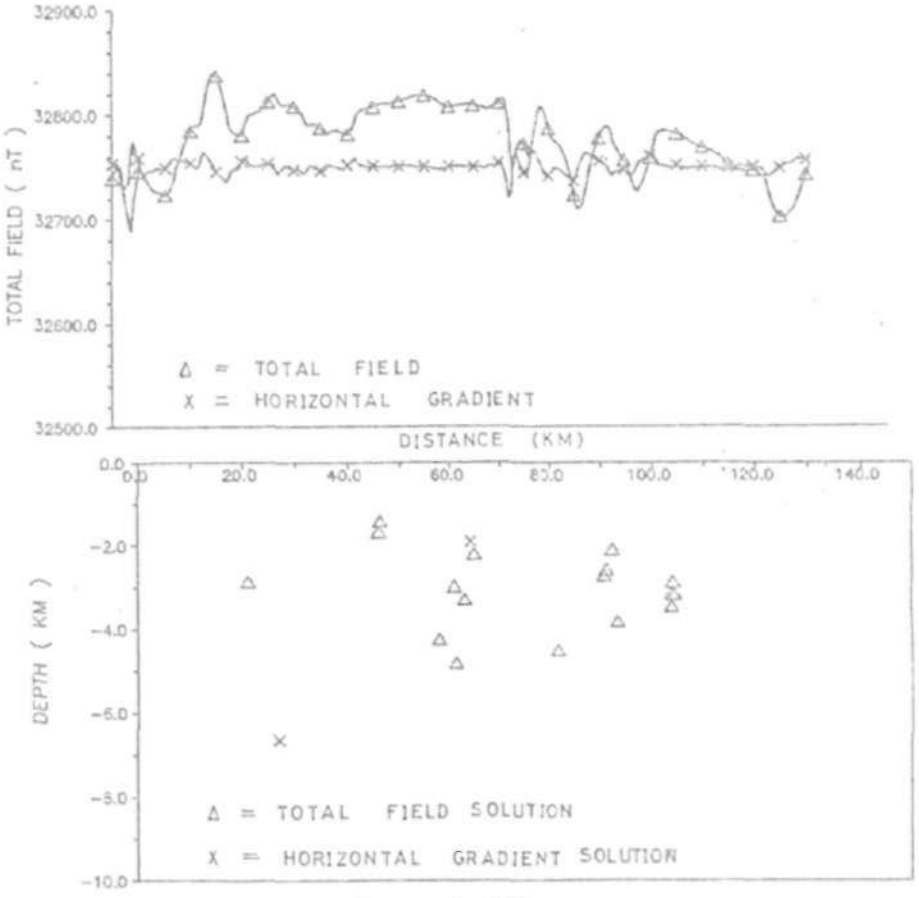
WERNER PROFILES FOR PROFILES L 189 & L 190



WERNER PROFILES FOR PROFILES L 180 & L 181

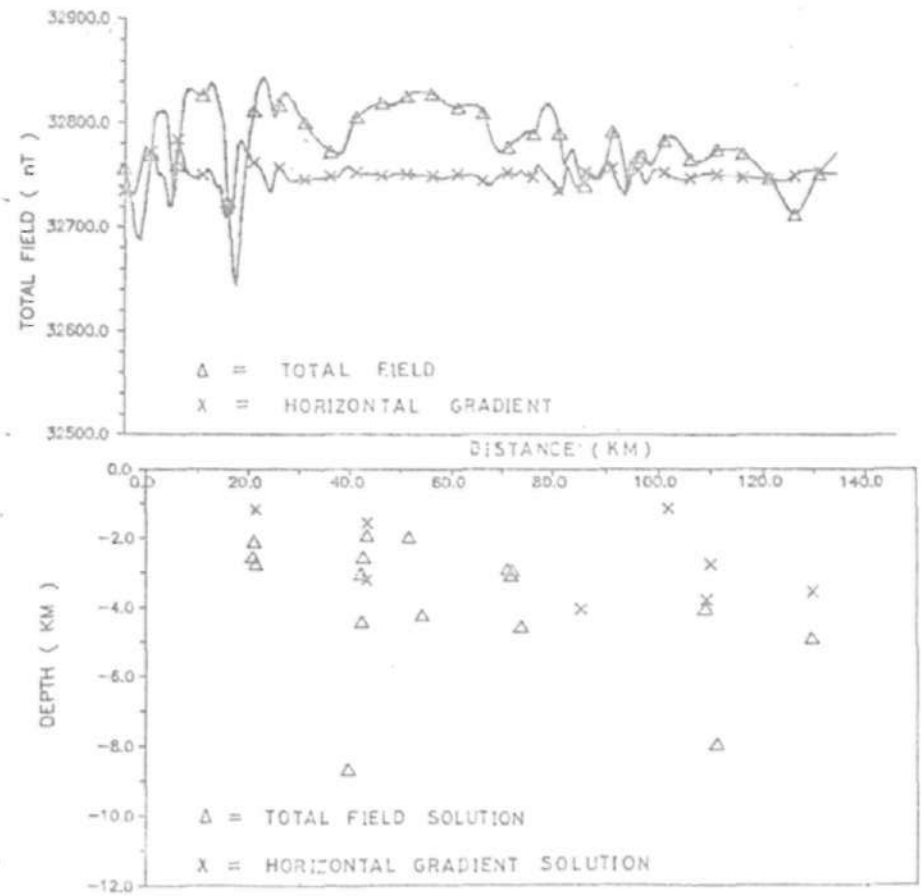


L 194

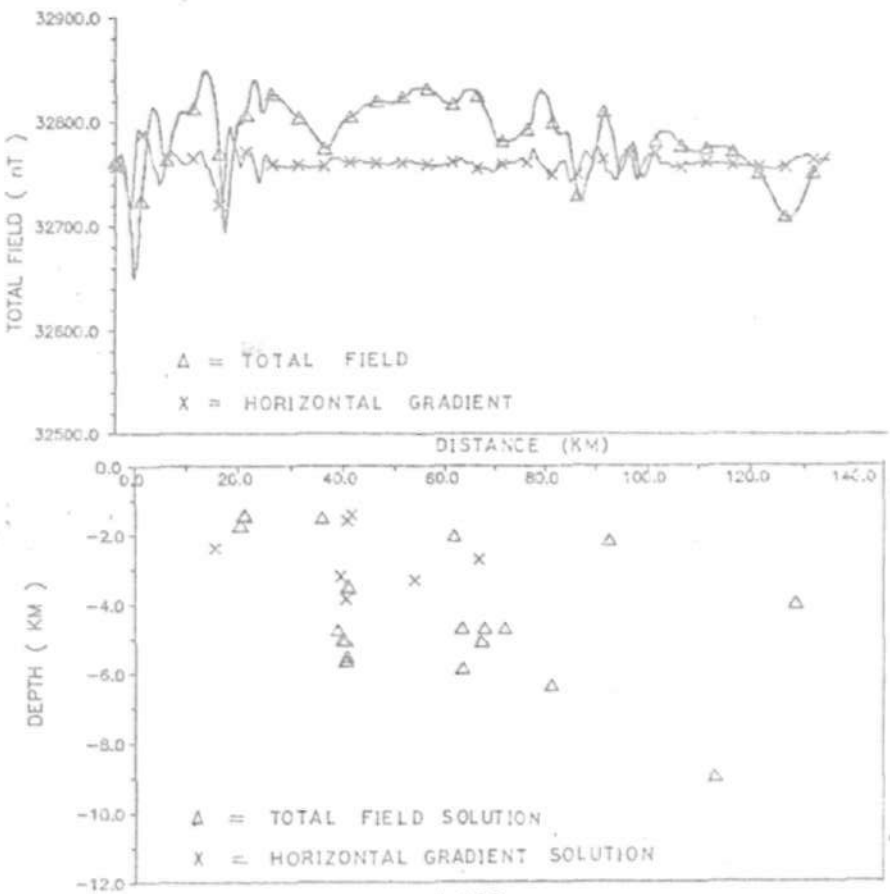


L 195

WERNER PROFILES FOR PROFILES L 194 & L 195

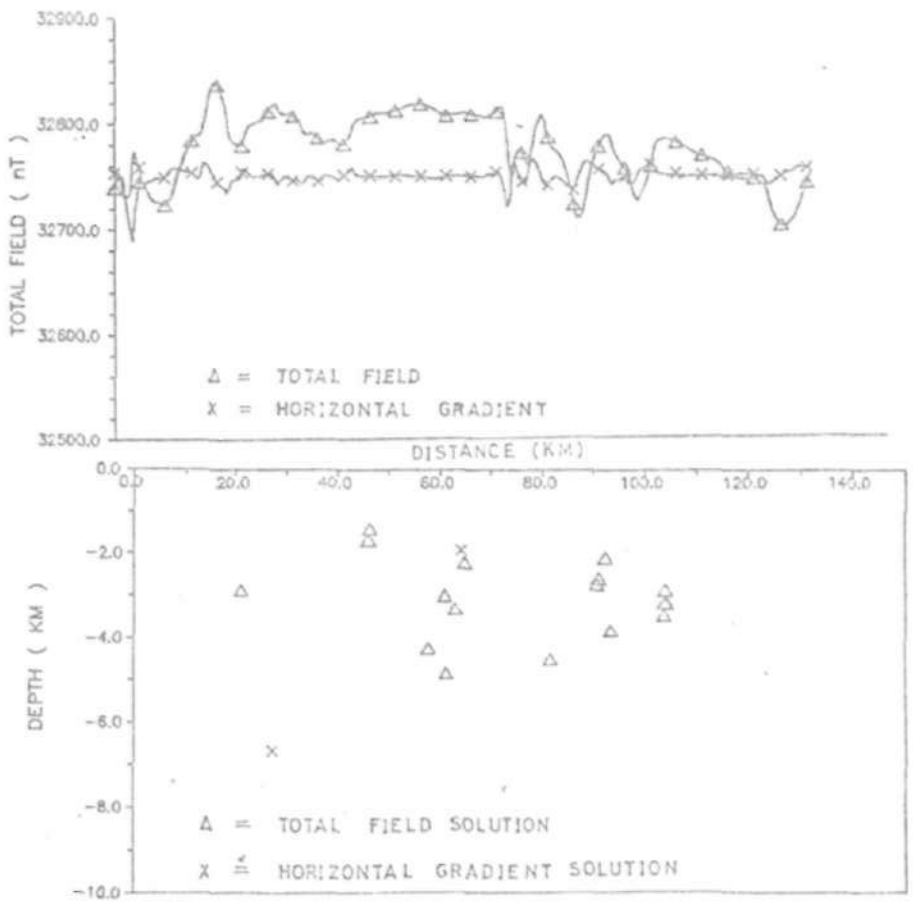


L 192

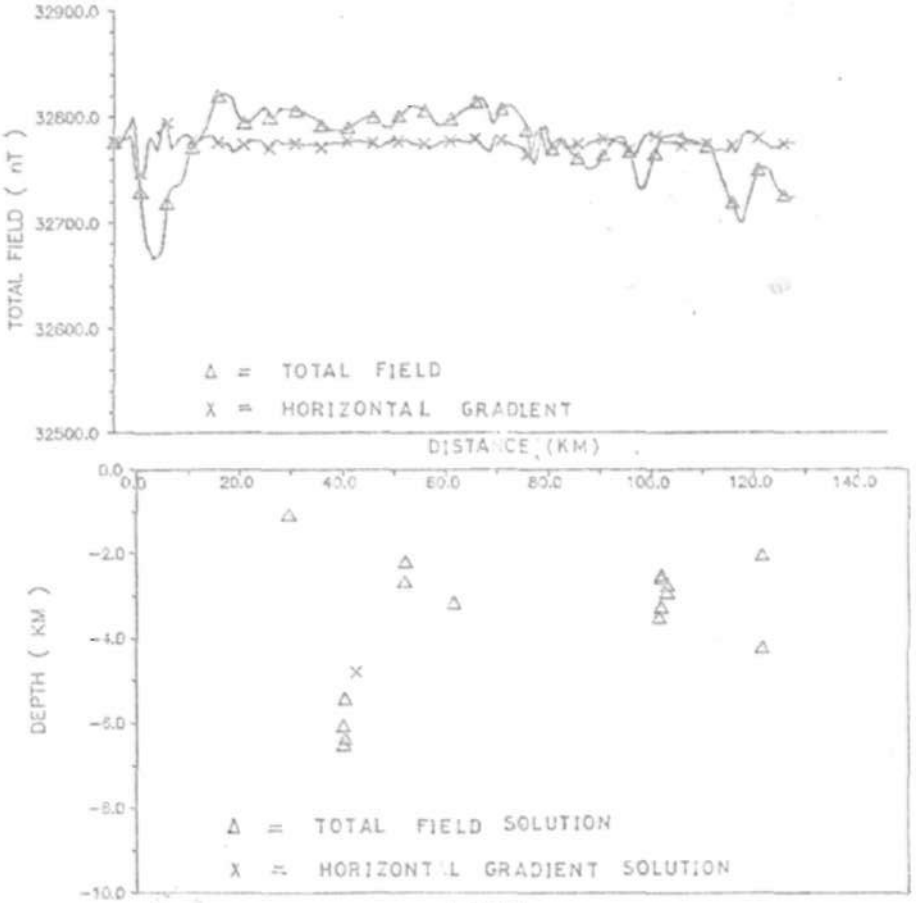


L 193

WERNER PROFILES FOR PROFILES L 192 & L 193

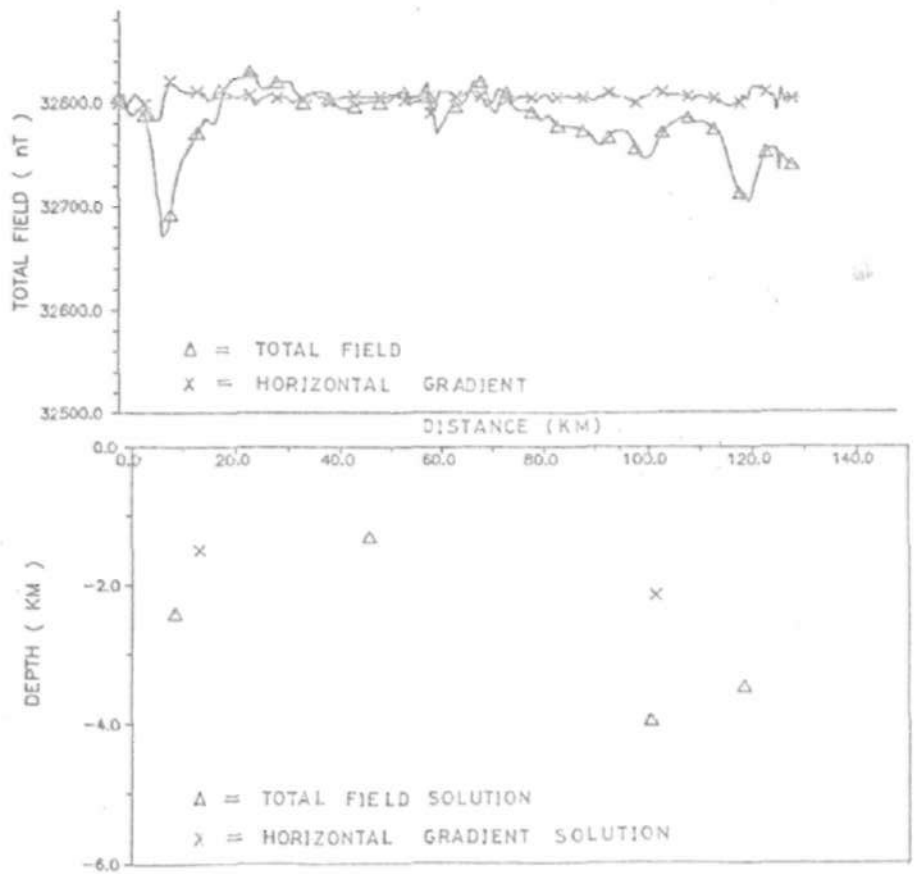


L 196

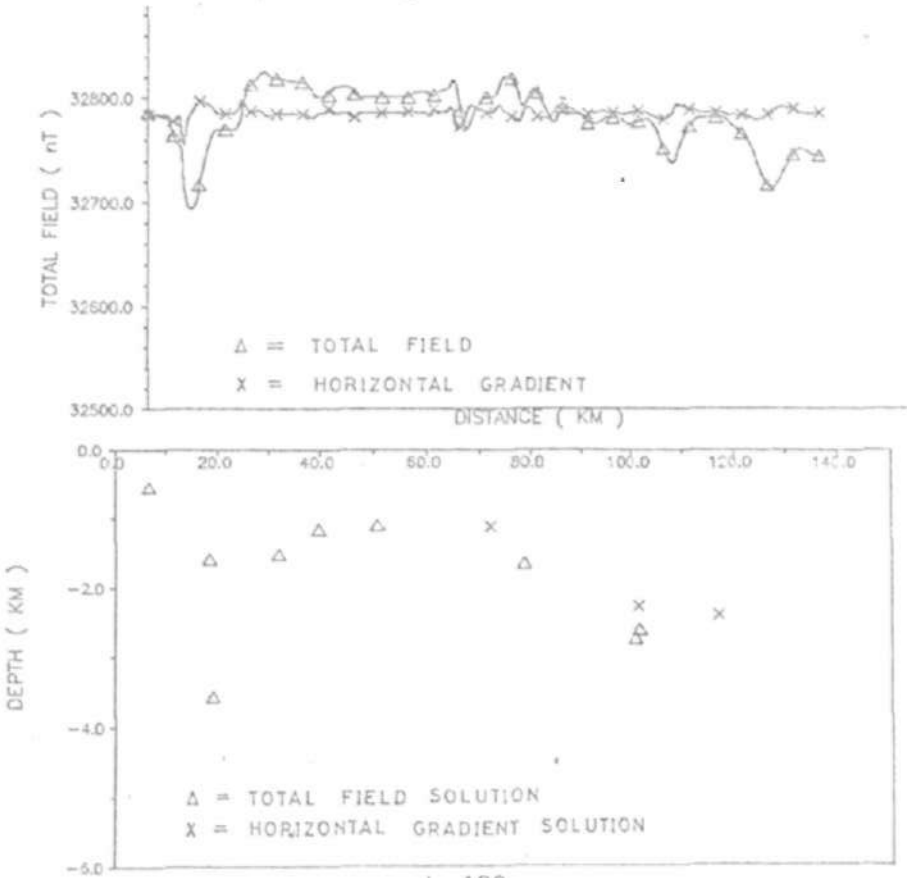


L 197

WERNER PROFILES FOR PROFILES L196 & L 197

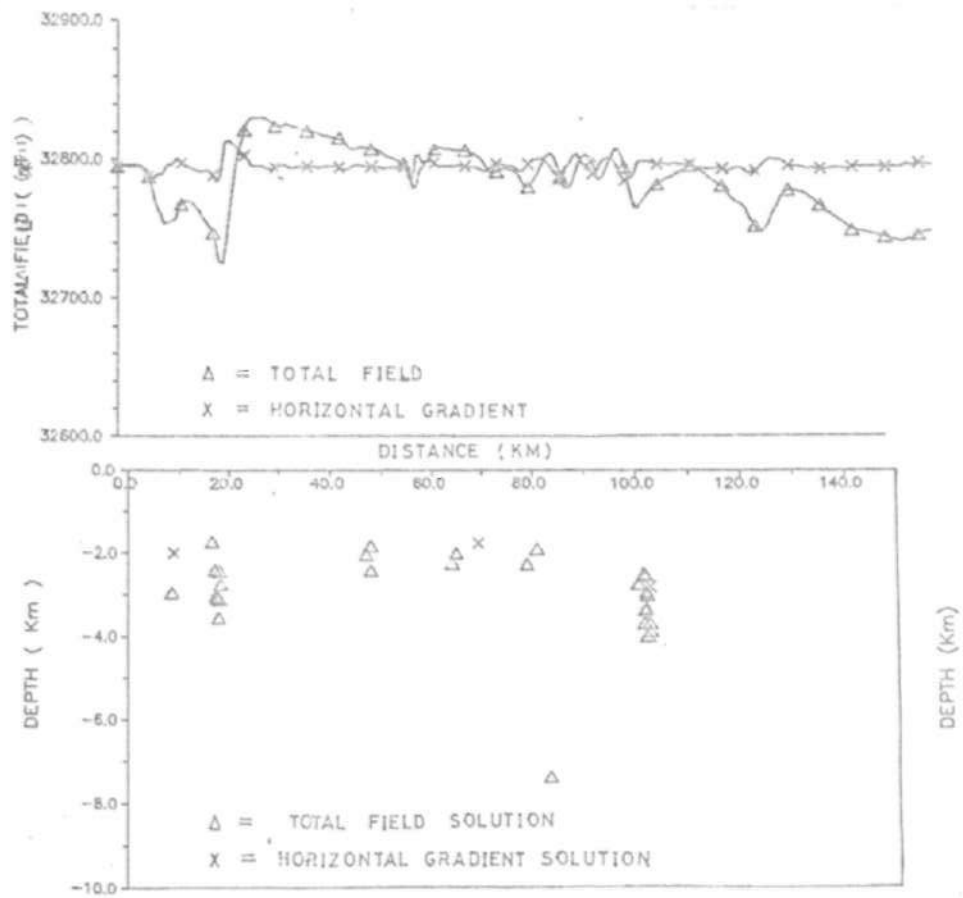


L 198

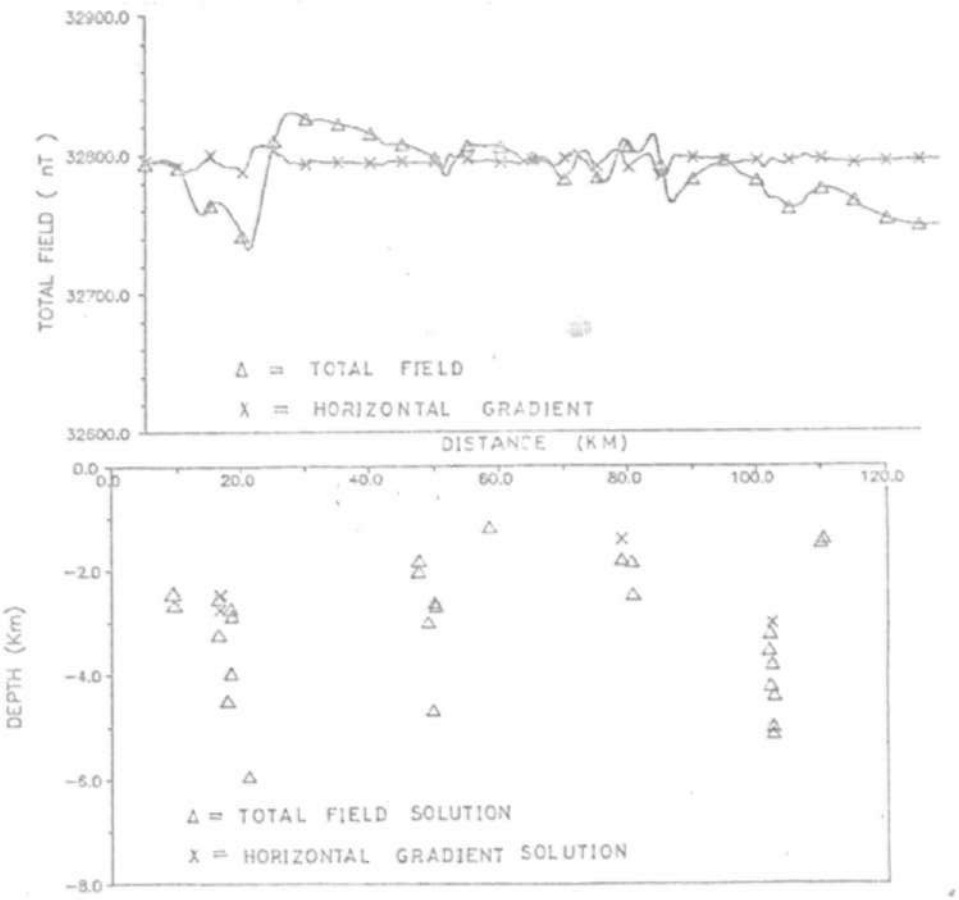


L 199

WERNER PROFILES FOR PROFILES L 198 & L 199

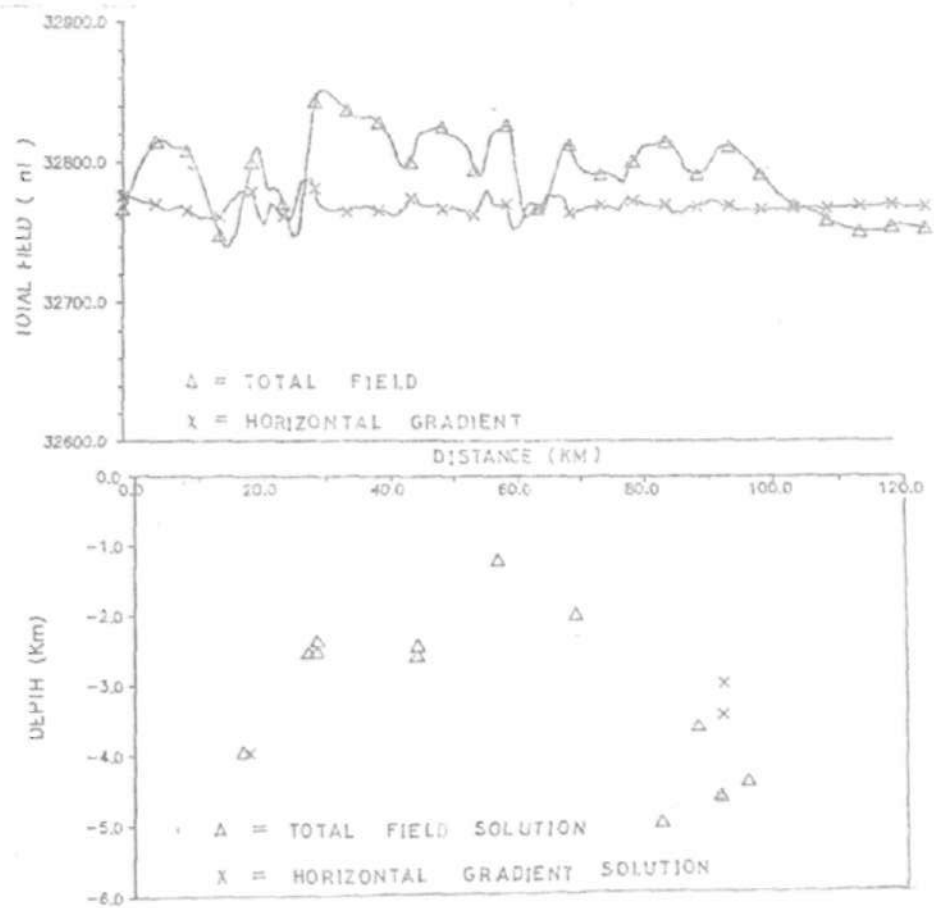


L 202



L 203

WERNER PROFILES FOR PROFILES L 202 & L 203



L 210 L 211

WERNER PROFILES FOR PROFILES L 210 & L211